Matthias Gilgien

External forces acting in direction of travel and their relation to energy dissipation in slalom

Masteroppgave i idrettsvitenskap
Seksjon for fysisk prestasjonsevne
Norges idrettshøgskole, 2008

Preface

The share of literature describing the kinetics of alpine skiing is limited in general, but especially for the discipline slalom. In recent kinematical studies energy dissipation, a measure for the quality of skiing, turned out having instantaneous statistical relations to key movement characteristics as well as to ranges of motion and performance measured in time. However scientific studies addressing these relations from a functional perspective, investigating how movement characteristics are related to kinetics and energy dissipation are lacking in the literature. The present study foremost attempts to broaden the knowledge about the external forces acting on the skier in direction of travel in the discipline slalom. Further the relation between these forces and energy dissipation is investigated to establish a basis for the description how movements are related with kinetics and energy dissipation.

The study is presented in a paper format, with an extended theory and methods chapter. The paper is not formatted to a certain journal, but is written as a stand alone part of the thesis. The title is: “External forces acting in direction of travel and their relation to energy dissipation in slalom.”

The code of the calculations behind this thesis is not attached as appendix, since it would fourfold the size of this document, but can be accessed by contacting the authors.

This thesis could not have been accomplished without help. I would therefore like to thank my main advisor Gerald Smith for the inspiring leadership, Robert Reid and Per Haugen for the outstanding support and company, Tron Moger, Håvard Tjørhom and Jonn Are Myhren for their contributions to the project, Matthew Brodie for the help regarding the wind drag computation, Olympiatoppen for the economical support to the project, Jostein Hallén, Robert Reid, Gerald Smith and Egil Johansen for having helped me to become an ordinary student at the NSSS and Ellen Moen for her extraordinary patience and support. Further I would like to apologize to my family and friends in Switzerland and Norway for having hidden myself in an office. I am looking forward to merge with your help from virtual to true alpine skiing.

Table of contents

1. Theoretical background

1.1 A science theoretical perspective on research in alpine skiing

Alpine skiing suffers as many other sports from the lack of extended scientific knowledge. Compared to science within an established paradigm, knowledge in alpine skiing regarding performance is quite pre-scientific to use the terms Kuhn had used to describe the different stages science is going through during its evolution (Chalmers & Lyngs, 1995). Among the important reasons for its pre-scientific stage is its limited economical value for the society, the time and resource consuming research process when choosing an analytical approach as it is the case in this project, the fast and ongoing development of equipment - and partly dependent on that - the fast development of new techniques. A lot of knowledge is therefore generated and carried by athletes and coaches, which form a kind of holistic sociological community in a Kuhnian sense (Chalmers et al., 1995) which is mainly interested in what Ryle described as "knowing how" (Chalmers et al., 1995). Due to the lack of appliance of extended scientific knowledge, this community is at risk to be lead by pseudoscientific convictions that may be grown historically and their work may suffer from vague definitions of the treated issues and their difficult transition into spoken language. The purpose of biomechanical studies regarding performance is therefore to combine this holistic knowledge with existent scientific knowledge to build models, derive and test scientific hypotheses and gain knowledge that is interesting both for the practitioner and science.

1.2 Description of the project frame

The thesis described here, is part of a PhD movement analysis project in alpine skiing that is going on since four years in the Department of Physical Performance at the Norwegian School for Sport Sciences (NSSS) lead by Robert Reid, Gerald Smith and Per Haugen. The development of the data acquisition methods, a good part of the data acquisition and a part of the data analysis were accomplished before the work for this thesis started. Two master theses (Tjørhom et al., 2007; Moger et al., 2007) have been written as part of the project and several conference proceedings are published (Gilgien, Reid, Haugen, & Smith, 2008; Reid et al., 2008; Reid et al., 2007; Tjørhom et al., 2007;

Haugen et al., 2007). Personally, I have been working in the project as a research assistant before I moved to the position of a Masters student.

1.3 Goal of the skiing mechanics project at the NSSS

The main vision of Robert Reid's movement analysis project is to broaden the understanding of skiing mechanics in general and its relation to performance. One area of specific interest is the tracking of the paradigm change that is about to happen regarding the choice of trajectories in competitive alpine skiing. Specifically more and more skiers have started to ski direct and short trajectories, forcing themselves to skid to a greater extent than the ones skiing longer and rounder carved trajectories but enabling them to use gravity as the accelerating force to greater extent during the phase of transition between the gates. At the time being it is unclear which strategy is superior in what skiing situation.

The gained knowledge is meant to be applied with the alpine skiing teams in Norway. Since it is not possible to cover all disciplines in such a project, the area of investigation is limited to the mechanics in slalom. Some of the gained knowledge might be general for skiing and can be applied to other disciplines, while other parts of it might be specific for velocities and turn radii typical for slalom.

1.4 Description of the mechanical model used for the NSSS project and the role of this thesis within it

The model we are working with is based both on holistic and skiing specific scientific knowledge. The holistic knowledge was gained by Robert Reid mainly by the mean of interviews with highly experienced coaches. The scientific knowledge was gained by the exploration of the existent scientific literature figure 1 shows its components written in the frames and its main relations indicated by the arrows. The left box contains key body movements which affect the ski loading and ski behaviour illustrated in the boxes more to the right. Ski orientation and loading interact with and determine the ski and centre of mass trajectory on one hand and on the other hand the mechanical energy, which is not transformed into kinetic energy and lost to the surrounding (energy dissipation).

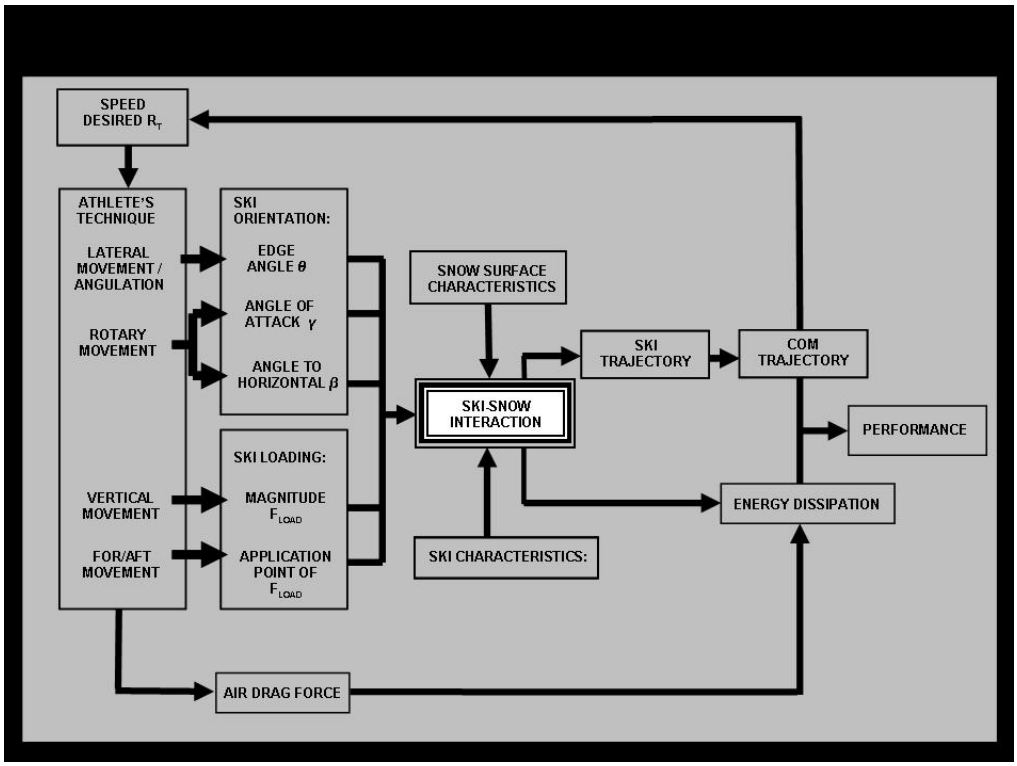

Figure 1: *The model the NSSS PhD project is based on.*

Energy dissipation and the COM trajectory together determine performance on one side, speed and turn radius on the other side, which lead to a new situation to be solved by the skier's technique. Since this biomechanical analysis is among few comparing several skiers kinematics on the same course, it represents one of the first opportunities to identify and quantify the importance of the components of this model as key aspects determining performance. As a first step in this identification and quantification process we started in spring 2007 hypothesising and testing the relation of the range of certain movements and movement patterns to performance measured in time. The published Master theses which were based on that work (Moger et al., 2007; Tjørhom et al., 2007) have shown statistical relationships between fore/aft dynamics, vertical movement and performance. The scientific value of these findings is limited, since a correlation between a movement and a time elapsed during a certain section in the course, does not establish cause and effect. We need therefore to go two steps further than that: First, we have already started to relate movement characteristics to energy dissipation (Supej, Kugovnik, & Nemec, 2005) instead of time. Energy dissipation can be calculated continuously and allows time series analysis, showing the instantaneous relation between movement and energy dissipation. Despite getting closer to the context of justification that way time series analysis still only describe how the two properties are

related in time. A more functional description of skiing mechanics is therefore needed to get close to a cause effect relation. In this project I therefore derivate external forces acting in the direction of travel from the kinematics and snow surface properties and relate them to energy dissipation. With this approach we hope to finally be able to describe the chain of acting elements from movements to forces and energy dissipation.

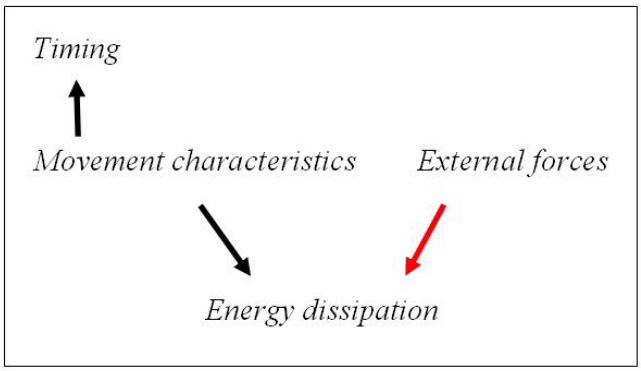

Figure 2: *Comparison of skiing characteristics and performance measures.*

1.5 Previous research in the NSSS project and the literature

The hypothesis I am questioning is part of the continuation of the identification process of key aspects regarding technique and performance in slalom as it is the focus of the PhD project. The analysis work that has been done so far in the project is partly published. A strong, negative, statistical relation between the range of vertical movement and performance measured in time was shown (Moger et al., 2007). On the same data a strong statistical relation was shown between the average fore / aft position during a turn cycle and performance measured in time (Tjørhom et al., 2007). Our own data shows, that fore / aft dynamics also have a reasonable relation to energy dissipation (Reid et al., 2008). Further we showed that energy dissipation has a relation to the centre of mass (COM) turn radius and is greater in the second part of the turn, probably due to greater forces acting in the lateral direction than in the first half of the turn (Gilgien et al., 2007). The findings from our data give reason to believe that the underlying kinetics play an important role in the relation between movement and energy dissipation.

Few studies exist regarding the complete modelling of the external forces acting on the skier in the direction of travel. Two studies did this for straight running situations (Kaps, Nachbauer, & Mossner, 2005; Kaps, Nachbauer, & Mossner, 1996) and four other for turning situations (Lüthi et al., 2004; Ducret, Ribot, Vargiolu, Lawrence, & Midol, 2004; Schiestl, Kaps, Mossner, & Nachbauer, 2006; Schiestl, Kaps, Mossner, & Nachbauer, 2005). None however related the external forces to energy dissipation. Due to that lack in the scientific literature and the belief that the study of the external forces acting on the skier are an important factor to understand skiing mechanics we selected this topic for my thesis.

1.6 The external forces acting on a skier

The external forces acting on the skier are illustrated in figure 3. Gravity ($F_{gravity}$) accelerates the skier downhill. The air-drag force (F_{drag}) de-accelerates the skier in the direction opposite to the direction the COM velocity vector is pointing. The reaction forces acting on the skis ($F_{reaction}$) have varying effects depending on the component. The component perpendicular to the skis creates centripetal force which changes the direction of the skiser's COM path. Together, $F_{gravity}$, F_{drag} , $F_{reaction}$ sum up to the total resultant force ($F_{resultant\_total}$) acting on the skier.

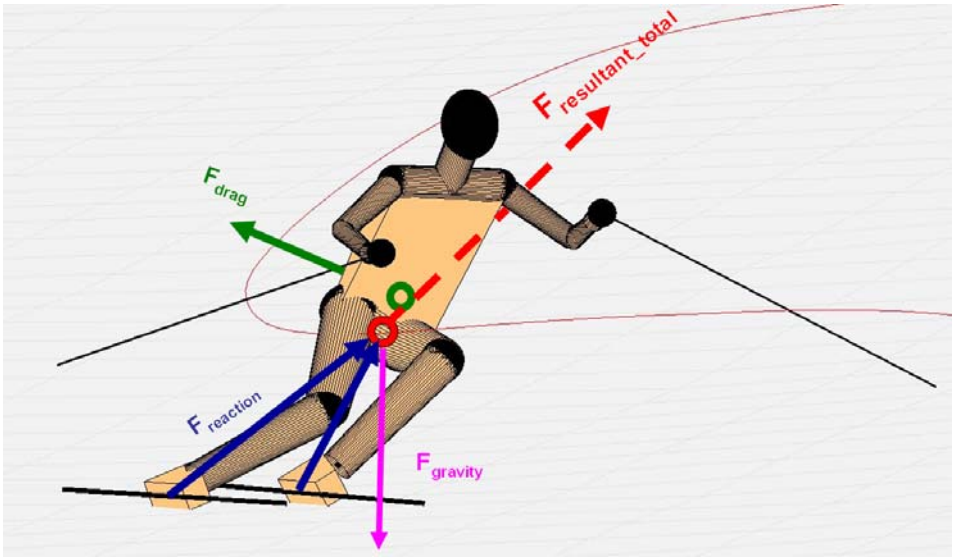

Figure 3: *The external forces acting on the skier.*

The total resultant force determines the COM trajectory of the skier. An illustration of the evolution of its size and direction is given in figure 4. The green line describes the COM trajectory. The blue lines represent the resultant force vectors acting on the COM at given moments in time.

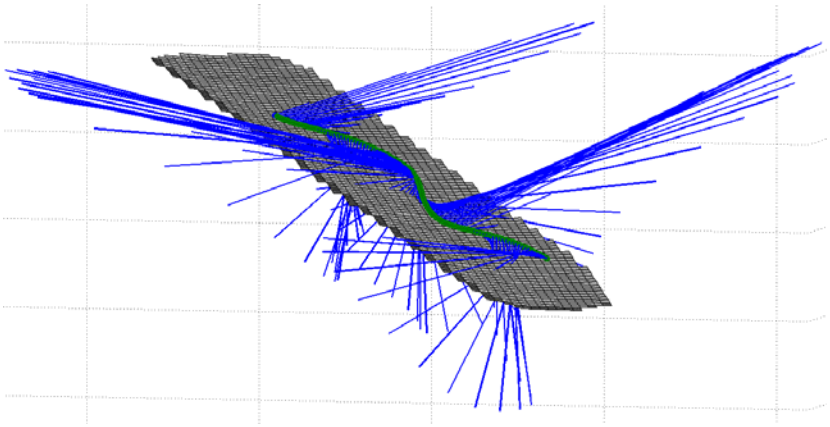

Figure 4: *The total resultant force vectors acting on the COM through 2 turns in blue. The green line describes the COM - trajectory.*

1.7 The external forces acting on a skier in the direction of travel

The quantification of the external forces acting parallel to the direction of travel of the skier is of interest since the knowledge about their size in slalom is very poor. Generally the external forces acting on the skier can be decomposed into their components in direction of travel. The centripetal force acts per definition perpendicular to the velocity vector and its projection onto the direction of travel is zero.

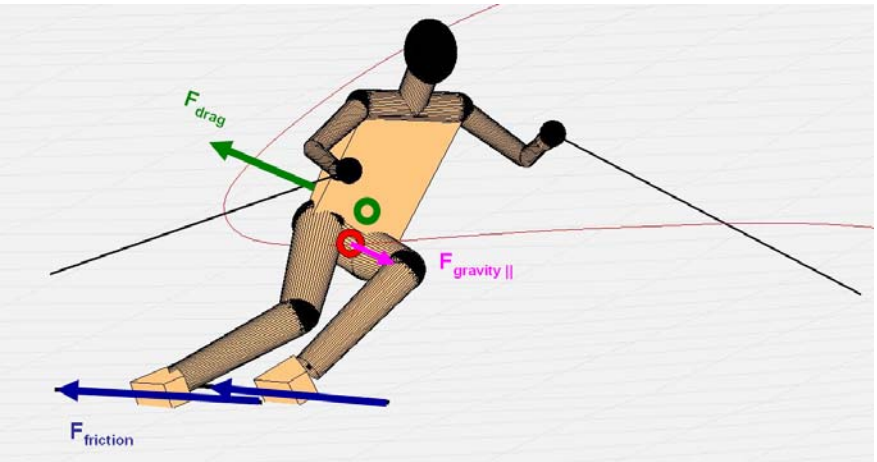

Figure 5: *The external forces decomposed into the forces acting in the direction of travel.*

The ski reaction force is decomposed into its component in the direction of travel ($F_{friction}$) and normal to the direction of travel ($F_{reaction\ \_|}$). The frictional force between ski and snow occur due to snow packing and kinetic friction (Howe, 2001). The air-drag force is acting in an opposite direction to the direction of travel. Its origin is dependent on the area distribution of the body and is thus generally not identical with the COM. For this study this difference was neglected and the air-drag force was assumed to act on the COM. Gravity can be decomposed to the component acting in parallel direction with the COM direction of travel. Similarly, the total resultant force can be decomposed in the component acting in the direction of the COM velocity vector.

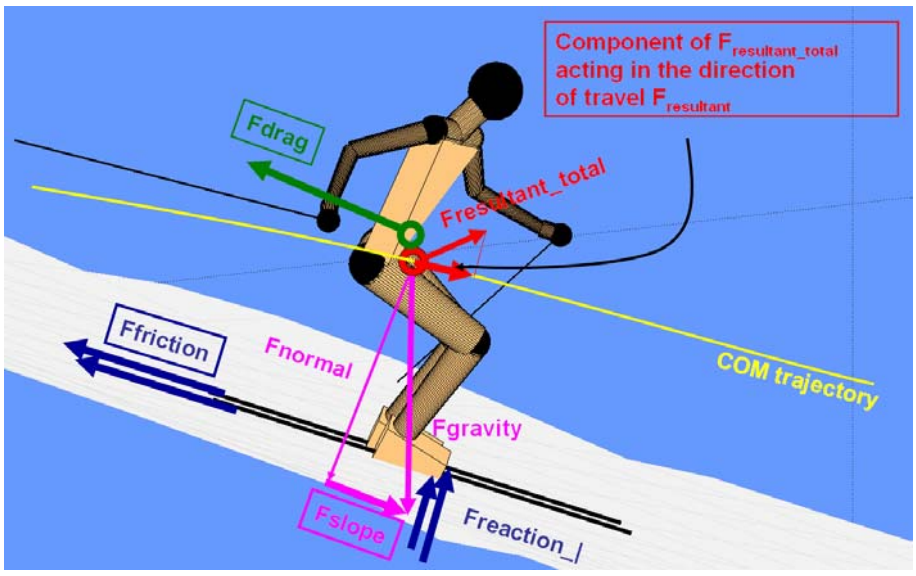

Figure 6: *The external forces acting in the direction of travel.*

The general nomenclature of the forces used in the study is the following: F_{slope} is the component of the gravitational force, pulling the skier down the slope along the direction of the velocity vector of the COM. F_{drag} is the braking force due to air resistance acting in the opposite direction to the COM velocity vector. $F_{friction}$ is the braking force due to friction in the ski snow interaction.

From the given data we are able to derive an approximation of the force acting on the skier down the slope (F_{slope}), the wind drag force (F_{drag}) and the total resultant force component acting in the direction of travel ($F_{resultant}$). But we are unable to calculate the dissipative force acting in the ski-snow interaction $(F_{friction})$.

To overcome this limitation, we access the size of that force with a difference equation:

$$F_{resultant} = F_{slope} + F_{drag} + F_{friction}$$

Equation 1

$F_{resultant}$ is equal to the sum of the forces acting on the skier in the direction of travel. Since we are able to compute all the forces except $F_{friction}$ we have to rearrange the above equation to access the size of $F_{friction}$.

$$F_{friction} = F_{resultant} - F_{slope} - F_{drag}$$

Equation 2

1.8 Choice of force models

Some studies have considered the skier as a point moving on the snow surface (Schiestl et al., 2006; Schiestl et al., 2005; Kaps et al., 1996; Kaps et al., 2005; Howe, 2001) or as a point travelling at constant vertical distance from the snow surface (Howe, 2001). In these studies, F_{slope} was computed as function of the surface inclination and the angle the skier was travelling to the gradient. Lüthi, Schiestl and Howe (Lüthi et al., 2004; Howe, 2001; Schiestl et al., 2006) however defined F_{slope} as being dependent on the movement of the COM. To understand the effect of different approaches on the external forces, we have computed three different. Their definition is given below.

1.8.1 Model 1: F_{slope} is dependent on the COM velocity vector inclination

This approach partly follows the suggestion of Lüthi, Schiestl and Howe (Lüthi et al., 2004; Howe, 2001; Schiestl et al., 2006). The resultant force is projected onto the 3-dimensional COM velocity vector, yielding the resultant force vector in the direction of travel $F_{resultant\_travel}$. Similarily, the component of gravity pulling the skier downhill is computed through projection of gravity onto the 3-dimensional COM velocity vector (F_{slope_COM}) as illustrated in figure 7.

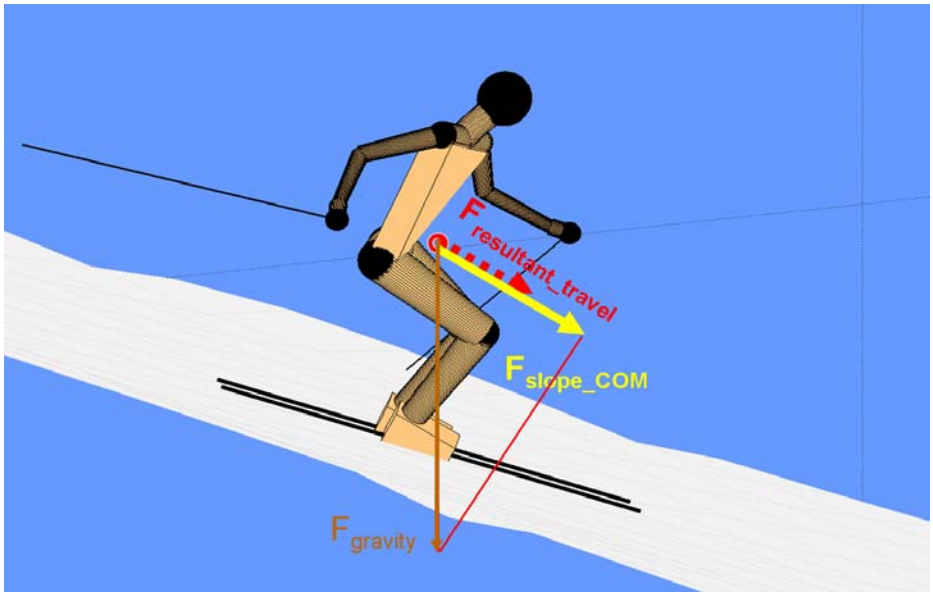

Figure 7: *Illustration of F_{slope} and $F_{resultant}$ definition for model 1.*

1.8.2 Model 2: F_{slope} is dependent on the slope inclination along the path of the COM

This approach follows the suggestion of Howe, considering the body as rigid and the COM travelling in a constant distance from the snow surface. Therefore F_{slope_COM} is determined by the inclination of the slope at the place the COM is projected on the snow surface and the angle to the gradient the projected COM instantaneously is travelling at as figure 8 illustrates. $F_{resultant\ ||}$ is calculated as the component of $F_{resultant\_travel}$ being parallel to the local snow surface. In contrast to model 1, this approach removes the effect of vertical movement normal to the local snow surface.

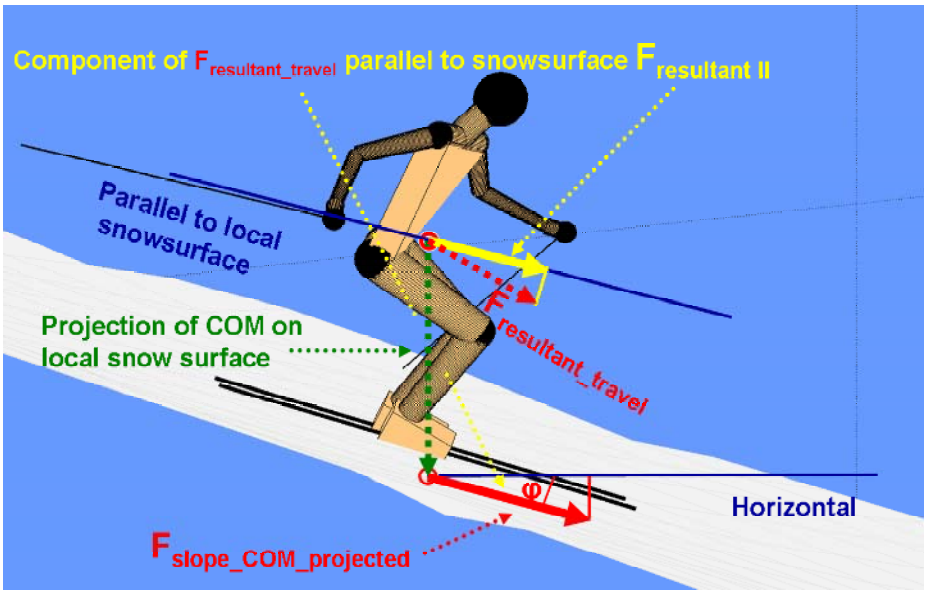

Figure 8: F_{slope} and $F_{resultant}$ definition for model 2.

1.8.3 Model 3: F_{slope} is dependent on slope inclination along the path of the skis

This approach assumes that F_{slope_SKI} is dependent on the inclination of the slope at the place the skier is in contact with the snow surface with his skis and the angle to the gradient he is travelling at (Howe, 2001). $F_{resultant\ II}$ is calculated as the component of $F_{resultant\_travel}$ being parallel to the local snow surface. In contrast to models 1 and 2. $F_{resultant}$ is not computed from the same point as F_{slope} consequently we have two points moving relative to each other. Figure 9 clarifies its definition.

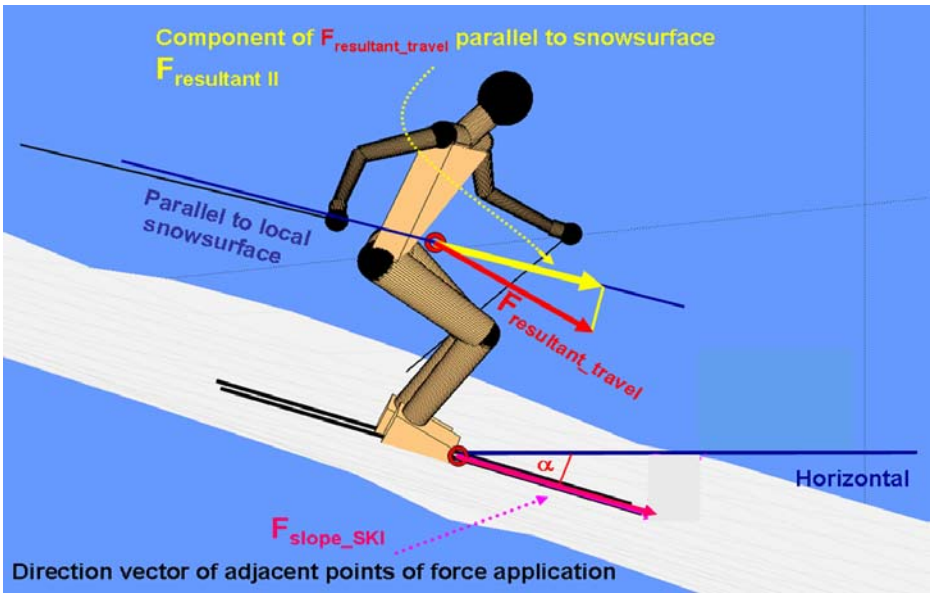

Figure 9: *F_{slope} and $F_{resultant}$ definition for model 3.*

1.9 Energy dissipation

As an instantaneous measure the energy was calculated the skier is dissipating to the surrounding through friction in the ski-snow interaction and wind drag. This measure was introduced in 2005 (Supej et al., 2005) and is used as a measure of performance instead of or along with timing. Energy dissipation *(E_{diss})* is defined as the COM's change in total mechanical energy *(ME)* per change in altitude per kilogram body mass (*m*). The total mechanical energy *(ME)* at each instant in time was calculated as the sum of skier potential energy *(PE)* and kinetic energy *(KE)*, knowing the center of mass altitude (*h*) and velocity (*v*) (Equation 1). Energy dissipation (E_{diss}) was then calculated as the change in mechanical energy per change in altitude per kg body mass (*m*) using finite central differences.

$$\begin{aligned} \mathrm{ME} &= \mathrm{PE} + \mathrm{KE} \quad [\mathrm{J}] \\ &= \mathrm{mgh} + \frac{1}{2}\mathrm{mv}^2 \quad [\mathrm{J}] \\ \mathrm{E}_{\mathrm{diss}} &= \frac{\Delta \mathrm{ME}}{\mathrm{m}\Delta \mathrm{h}} \quad [\mathrm{J}\cdot\mathrm{kg}^{-1}\cdot\mathrm{m}^{-1}] \end{aligned}$$

Equation 3

Both original data (Supej et al., 2005; Supej, Kugovnik, & Nemec, 2004; Supej, 2008) and our data show negative E_{diss} values around turn transition. Supej had referred to muscular work being the reason for that to occur without specifying its characteristics. To achieve a better understanding of the phenomenon, it could be useful to see, what the characteristic body motion during that period of the turn cycle is.

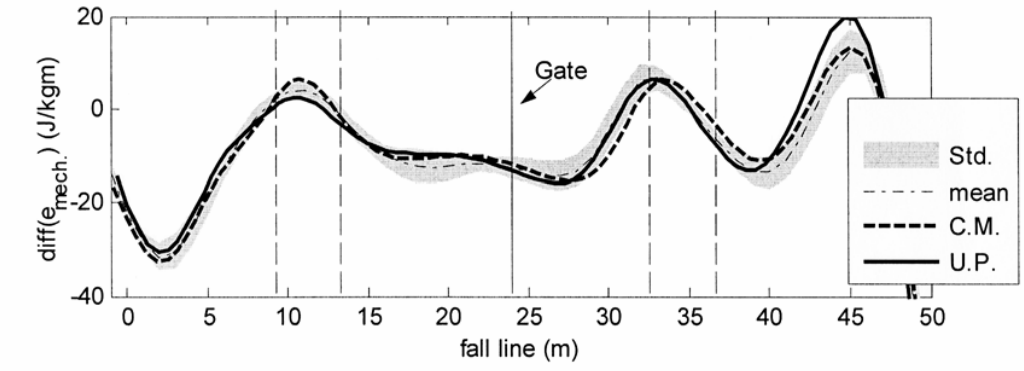

Figure 10: *Energy dissipation defined as being negative, when energy is dissipated to the surrounding and positive when gained, due to muscular work for two turn cycles. The dashed vertical lines indicate the turn transition. The solid vertical lines show the*

gate position. From: "Differential Specific Mechanical Energy as a Quality Parameter in Racing Alpine Skiing." By Supej, M., 2008, Journal of Applied Biomechanics, 24, p. 124, Copyright 2008 by Human Kinetics. Reprinted with permission of the author.

1.10 Research questions

Since the forces acting in parallel to the direction of travel have not been computed before in the slalom discipline, we mainly want to find their description for the two captured slalom turns. The specific research questions for this thesis are:

Question 1: What is the course and size of the external forces acting on the skier in the direction of travel through two slalom turns?

Question 2: To what extent do the wind drag force and the braking force in the ski snow interaction contribute to the total braking force?

Question 3: How are the braking forces related to energy dissipation?

Question 4: Is there a relation between the negative energy dissipation values at the transition between turns and propulsive forces acting on the skier?

Question 5: If there is a relation between energy dissipation and propulsive forces at the turn transition, what are the movement characteristics during that phase and do they give reason for the propulsion?

2. Methods

2.1 Timecourse of the datacollection

The data collection was accomplished in a slope called "Varingskollen" in Nittedal 15 km northwest from Oslo on April 11th, 2006. Due to the typical spring temperatures, the slope was prepared by repeated side-slipping. The control points for the photogrammetric analysis were setup towards the evening of April 10th 2006, when the snow started to freeze. As soon as their carriers were frozen and not at risk of moving anymore the position of the control points as well as the geomorphology of the snow surface were captured with a theodolite.

2.2 Weather and snow conditions

During the data collection in the morning between 8h and 11h the temperature ranged from 5 ºC to 7 ºC and the snow surface was compact and hard during the whole data collection due to a cold night with minimal temperature of -5.8ºC. The weather was sunny on both April 10th and 11th and close to wind still.

2.3 Population

Six male skiers of the Norwegian Europa Cup team in the age range from 17 to 20 years (average: 18.3) were chosen. Their position in the official ranking of the international skiing federation (FIS) ranged from 112 to 500 corresponding to 13,4 to 32,4 FIS points at the time the study was conducted. With respect to their age classes, they were among the 6 best worldwide.

2.4 Timing and selection of trial

A photocell timing system (Microgate S.R.L. Bolzano, Italia) was used to measure times in a section directly before (TS 1), during (TS 2) and adjacent (TS 3) to the area of investigation by putting photocells at the entrance, several meters before, at the exit and several meters after the area of investigation.

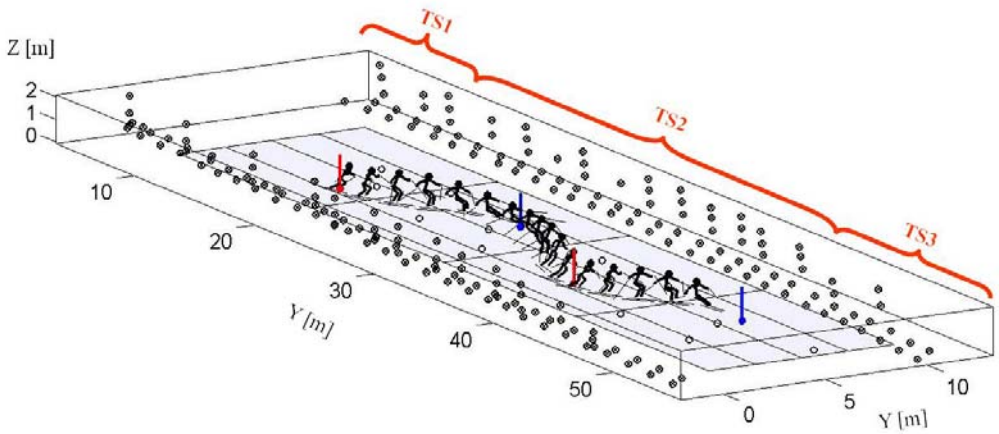

Figure 11: *Schema of the area of investigation with the timing section TS 1-3.*

The timing was used to select the best but at the same time consistent performances out of three runs per athlete. Specifically the times needed for the passing of the area of investigation (TS 2) was correlated with the time needed from the first photocell the skiers passed and the last one, which was placed several meters after the area of investigation. The consistency criterion was taken into consideration to make sure the athletes were performing in unexaggerated manner during the time their movements would be analysed. Exaggerated movement would lead to findings which do not represent the manner of skiing which can be maintained through a whole course.

2.5 Area of investigation and course setting

The area in which the movement analysis was accomplished was about 40 meters long and 20 meters wide and situated in the upper halve of a longer slalom course. With the placing of the investigation area within a longer course , we tried to avoid the athletes skiing in an exaggerated manner through the turns in the area of investigation. The course was set with inclined distances between the gates of about 10 meters and an offset across the hill of 3 meters by the coach of the European Cup team of the Norwegian skiing federation. The area of investigation covered 4 gates. In the area of investigation, the slope was tilted about 19º with the gradient in an angle to the main direction of the course of 14.5º to the right, when looking into the downhill direction. The terrain before and after the area of investigation had about the same characteristics as one can see from figure 12.

***Figure 12**: The area of investigation.*

2.6 Setting of photogrammetrical controlpoints

208 control points were placed along the two sides of the course. To enable the calibration of the whole volume the skiers would ski through, the control points were set up in different vertical locations spanning a volume of approximately 40 x 20 x 2m. 117 control points made of foamed rubber were placed in a zig-zag pattern approximately 15 cm above the snow surface. 80 control points made of tennis balls were mounted on 32 gates and placed at heights ranging from 80 to 220 cm above the snow surface. In addition to these points placed at a distance from the course, 11 control points were placed on the inside of the gates in form of tennis balls mounted on foamed rubber sticks. The two parallel lines of control points along the course were set in a distance of 11 meters across the hill from each other, far off the course to avoid visual disturbance of the skiers and to allow re-setting of the course to a course with 13m inclined distances between the gates which were used for a following study as it is apparent from figure 13. Since the accuracy of photogrammetry is increased the closer the calibration points are placed to the area the athletes ski through (Shapiro, 1978; Chen, Armstrong, & Raftopoulos, 1994) the above mentioned 11 control points were placed in a zig-zag pattern on the inside of the gates.

***Figure 13**: Schematic setup of control points (Picture is from another datacollection).*

2.7 Surveillance of the control points and the snow surface

The positions of the control points were measured with a theodolite (Sokkia Set 2BII, Sokkia Co. Ltd. Kanagawa, Japan) which was positioned near the track. To enable a stable positioning of the theodolite in the snow, the tripod was dug in salted and watered snow. The measuring process was not started before the tripod was frozen in the snow due to the falling temperatures towards the night. The height and the vertical- and horizontal orientation were controlled frequently during the measurement process (after every fifth measurement) to avoid a systematic drift over time in the measurement system. The reference direction was chosen to an iron pillar across the hill. The distance to the control points was measured by holding a reflector to the side of the point and the horizontal and vertical direction by screwing the reticle into line with the centre of the marker. These measurement data were saved both manually and in an electronic data logger, which was directly connected to the theodolite. In addition to the control points the geomorphology of the snow surface was captured with the same method. The distance to the snow surface was measured by the mean of a reflector and the direction by screwing the reticle to where the reflector touched the snow surface. Since the snow surface was pretty uniform the points were captured with a distance between of approximately 1.5 meters. The surveillance setup is given in figure 14.

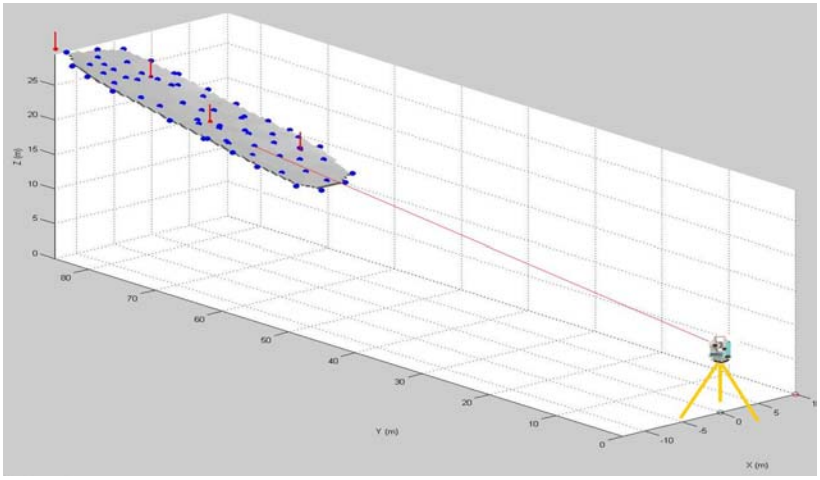

Figure 14: *Schematic illustration of the surveillance setup*

2.8 Filming process

The filming of the skiers was accomplished by four DV cameras. Two of them were Sony TRV 950, one was a Sony TRV 901 and one was a Canon DM- XM2 E. The minimal shutter speed was set to 1000 Hz since due to favourable light conditions and to obtain sharp images the capture frequency was set t 25 Hz and later PAL – deinterlaced to 50 Hz. The direct linear transformation method which was used for the photogrammetrical analysis requires that 6 control points are visible in the image. Therefore the zoom was set fixed to ensure 6 points were visible in the camera pictures. As it can be seen from the figure below, the cameras were placed in a few meters from the investigation area and were panned and tilted to follow the skiers to cover as many control points as possible. The cameras were far enough from the course to make sure the whole skier and as many control points as possible could be captured even when the skier passed close by the camera. The cameras were positioned at the beginning and end of the area of investigation, as illustrated in figure 15, to ensure most possible camera angles would intersect close to 90˚, which is favourable for the accuracy with the direct linear transformation method (Shapiro, 1978; Wood & Marshall, 1986).

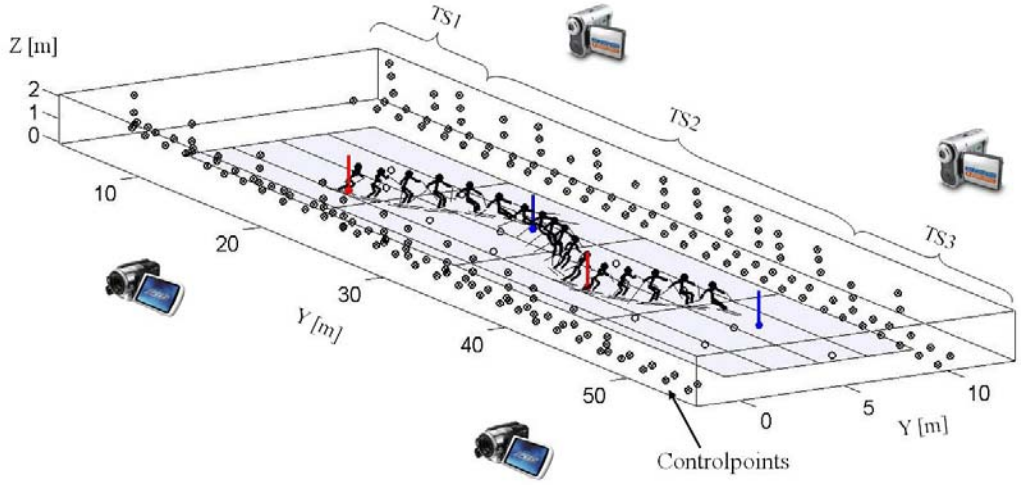

Figure 15: *Schema of the filming process, the control points and the timing sections (TS).*

2.9 Camera synchronisation

Due to lacking access to hardware genlock cameras, the synchronisation of the cameras was post processed (Pourcelot, Audigie, Degueurce, Geiger, & Denoix, 2000) using an algorithm that accommodates panning cameras. The method calculates the phase shift between cameras by minimising the errors in the reconstruction of a point in motion. The pole tips were chosen for that purpose, since they are well defined and can therefore be digitised more precisely than other points on the skier. Further the pole tips were chosen because they are moving rapidly in both the object and image spaces. Due to the cameras following the skier, the pole tips are some of the only points actually moving rapidly in the image space. One camera is chosen to be the reference camera and the others are synchronized with their individual phase shift relative to the reference camera by cubic interpolation. The interpolation was optimized according to minimize the non control point error.

2.10 Direct linear transformation method

The direct linear transformation method (DLT) was used to reconstruct a spacious model of the skiers from the two dimensional film data. (Abdel-Aziz & Karara, 1971) were the first ones describing the DLT method ((Shapiro, 1978; Wood et al., 1986). Later the DLT method was adapted by (Mossner, Kaps, & Nachbauer, 1996; Nachbauer et al., 1996) to the specific needs of alpine skiing by allowing to zoom, tilt and pan

cameras. The DLT method in more detail: The direct linear transformation method describes the reconstruction of an object in three dimensional space (objectspace) from at least two two-dimensional pictures (image space) taken from different positions. The transformation-measures between the image- and the object space are based on the solution of a system of equations which describes the relation between object- and imagespace. The equation describing the calibration process contains 11 unknowns for which the equation system can be solved for if the coordinates of at least 6 points in both image- and objectspace are known. The over-determined system of equations is solved by a least-square method. The 11 unknowns describe the camera constants and orientation. They are different from frame to frame in case the camera is tilted and panned, as it was the case in this investigation. For technical (Schiestl, 2005) and economical reasons the control points in every second image only were digitized and the camera constants calculated, while the camera constants of the intermediate images were interpolated. The camera constants were filtered with a 2^{nd} order low-pass Butterworth filter with a cut-off frequency of 15Hz.

The accuracy of the calibration is increased with an increasing number of control points. Shapiro (Shapiro, 1978) found that the amount of control points in the volume should range from 12 – 20 points while (Chen et al., 1994) showed that their amount should range from 16 – 20 to attain optimal accuracy. In the current investigation the average number of control points per image was 29 and the minimum 14 (Reid et al., 2008). The accuracy is further dependent on the distribution of the control points in the investigation volume. An evenly distribution promises a continuous level of accuracy over the whole volume. The third factor the accuracy of the DLT method is dependent on is the coverage of the whole volume the athlete is moving in. If the athlete extends the calibrated volume, extrapolation will cause severe problems with the accuracy (Chen et al., 1994; Wood et al., 1986).

The reconstruction of a point in object space is accomplished by the least-square solution of its quasi intersecting rays which pass through their respective points in the image spaces and focal points of the different cameras.

2.11 Digitalisation and construction of a skier model

The captured DV film material was imported by DartFish (Fribourg, Switzerland) and an Indeo Codec 5.0 to Matlab (TheMathWorks, Natick, USA). In Matlab the digitalisation was accomplished by a tool specifically developed for this purpose by Robert Reid illustrated in figure 16. The resolution in the digitalisation tool was 720x576 pixels.

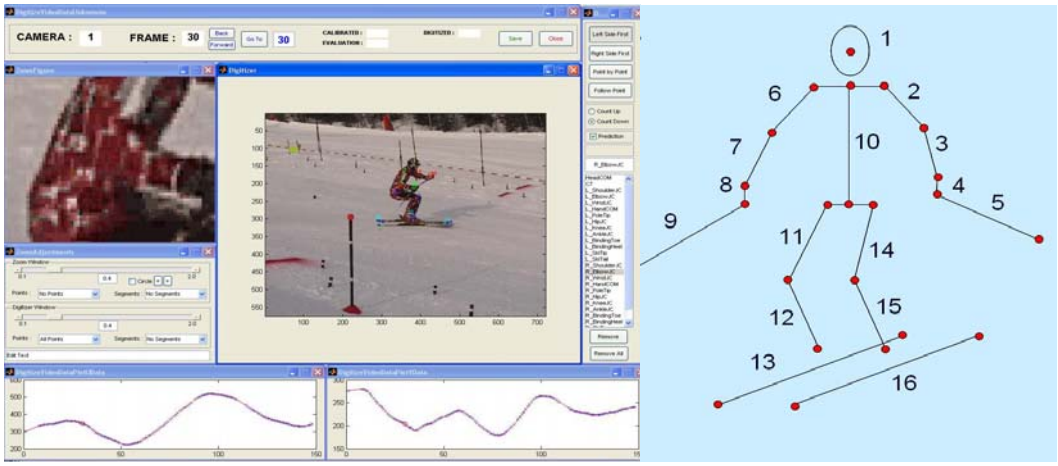

***Figure 16**: Digitalisation software specifically developed for this project by Robert Reid on the left side and an illustration of the skier model with joint centres in red and segments on the right hand side.*

The joint centres of the shoulder, elbow, wrist, hip, knee and ankle were digitised as well as the centre of the head, the centre of the hand, the ski tip and tail and the pole tip. The right hand side of figure 16 shows a simple model of the skier consisting of 18 segments between the reconstructed joint centres, skis and poles is shown in the picture below. The points 27 and 28 were calculated based on the shoulder and hip joint centres.

In case a point could not be reconstructed because it was out of site for three cameras, its position in object space was interpolated with a cubic spline function from the preceding and adjacent points. These objectspace position data were filtered with a 2nd order low-pass Butterworth filter with a cut-off frequency of 10Hz.

2.12 Accuracy of the motion capture method

The methods accuracy was estimated in three different ways. In a first approach the control points placed at the inside of the turn and close to the gates were used to predict the DLT accuracy. They were left out for the calibration of the images and their position predicted from the calibrated images and compared to the values of the terrestrial position measurements with the theodolite. The root mean square error (RMSE) for the prediction of non-control points was 15mm (n = 1621 predictions for 6 trials) (Reid et al., 2007). The non-control points close to the gates were finally used in the calibration of the images to increase the number of points accessible for calibration to increase the accuracy of the calibration. Therefore the true accuracy is better than the above reported. As a measure for the digitizer's ability to hit the true centre of the joints, segment lengths were calculated from the object space coordinates. The pooled standard deviations ranged from 9mm (hand/pole) to 14mm (leg) with the amount of measures per segment at around 1480 (Tjørhom et al., 2007). As a third measure for validity of the method, the true segment lengths of 4 athletes were compared to the calculated segment lengths by the mean of the root mean square error. The results are given in the table below from (Tjørhom et al., 2007).

***Table 1**: The segments RMSE and number of predictions.*

Segment	Upper arm	Under arm	Thigh	Leg
RMSE [mm]	12,46	12,01	31,33	16,51
N	750	750	749	749

2.13 Calculation of the centre of mass

Many calculations in this study are based on the position of the centre of mass. For economical, anthropometrical and technical reasons the body segment parameter model of Zatsiorsky (Zatsiorsky & Seluyanov, 1985; Zatsiorsky, 2002) with the adjustments from Leva (de Leva, 1996) was chosen. The equipments mass was added to the respective segments and the trajectory filtered with a 2nd order low-pass Butterworth filter with a cut-off frequency of 5Hz, since velocity and acceleration were derived from the COM.

2.14 Coordinate systems

In the surveillance process the snowsurface was captured with a theodolite on an uneven grid with sidelength of about 1.5 meters between the 82 points. Their position description in polar coordinates in which they were logged during the surveillance process was transformed into a cartesian coordinate system by the mean of standard trigonometry. The origin of the Cartesian coordinate system is still at the vertical projection of the theodolites centre on the snow surface. The X and Y axis of the Cartesian coordinate system were chosen to be approximately parallel to the area of investigation to allow the description of the slope's leaning in terms of axis of the so called theodolite coordinate system. To simplify the calculation of characteristic movement measures such as vertical dynamics for example, the theodolite coordinate system was transformed by the mean of Euler rotations into a coordinates system having a least-square plane computed on the captured points on the snow surface as X-Y plane and the normal on that plane as the vertical Z axis. This coordinated system was named course coordinate system.

2.15 Digital terrain modelling

2.15.1 Least-square plane model

As a first approximation of a snow surface a least-square plane was calculated into the points describing the geomorphology of the snow surface. The size of the residuals of this model was 6.4cm in average and 27.1cm maximally. We will see later when we describe the calculation of the external forces that this approximation is too rough to allow a proper derivation of the force pulling the skier down the slope in the direction of travel. Therefore a more complex model was necessary to be built. Figure 18 illustrates the residuals of the captured points to the least – square – plane.

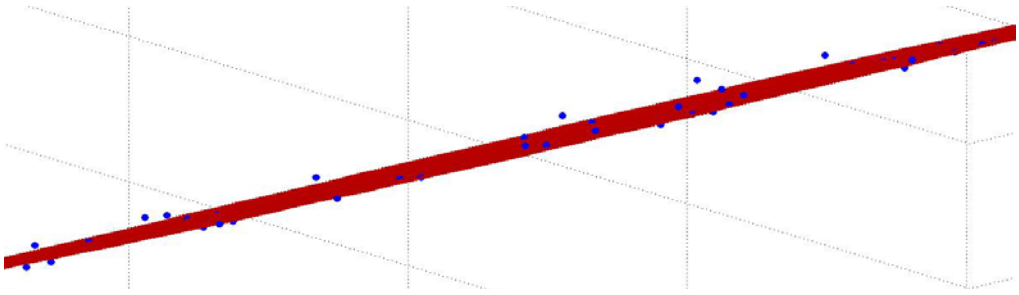

Figure 17: *A sheer plan view on the least-square plane model in red and the captured points in blue.*

2.15.2 Triangulation based model

To build up this model the captured points were triangulated with the method of Delauney (de Berg, Otfried, van Kreveld, & Overmars, 2008) to a surface consisting of triangles that's sides connect the captured points on the snow surface. In case the number of points to triangulate is too big to be accomplished by hand, the Delauney algorithm is the most common used algorithm for automated triangulation (de Berg et al., 2008). With the method of Delaunay the points are triangulated such that no point is inside the circumcircle of any triangle. The method further maximizes the minimum angle of all the angles of the triangles in the triangulation. That way the method tends to avoid acute-angled triangles. Figure 19 illustrates the process of triangulation. The programming of the triangulation was accomplished in Matlab as all the other calculations in the digital modeling part of this study. The shortcoming of this approach is that the surface spanned by the triangles is not continuous in the first and second derivative across the area. Regarding the calculation of the force pulling the skier down the slope this shortcoming can cause problems. Therefore a third model was built which provides continuous first and second order derivatives.

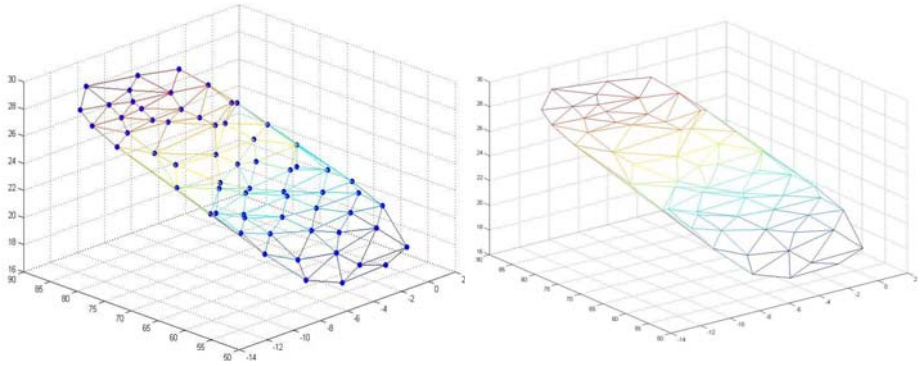

Figure 18: *The triangulation of the captured points on the snow surface on the left side and the triangulation based model on the right-hand side.*

2.15.3 Smoothed triangulation based model

The construction of a digital terrain model that enables the derivation of local gradients area-wide was accomplished by smoothing of the above described triangulation based model. In a first step a rectangular grid with side length of 40 cm was plant in the above described least-square plane as a reference frame for the smoothing of the triangulation based model.

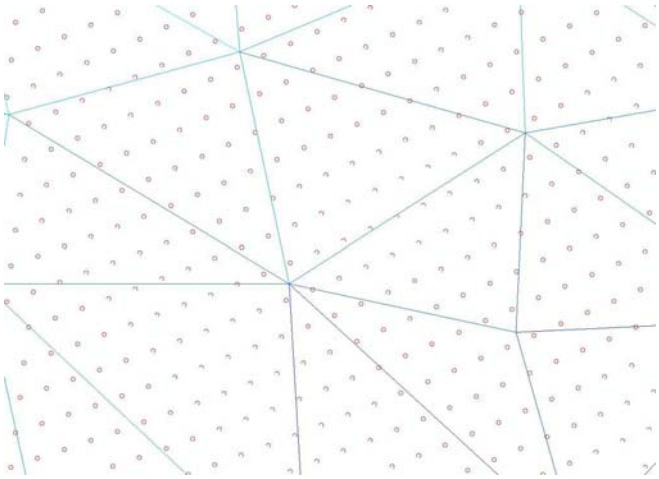

Figure 19*: The triangulation in blue and the 40 cm gridpoints shown in red.*

The smoothing of the triangulation based model was conducted by the interpolation of the captured data points with a smoothing function on the rectangular grid as a basis. Since it is known from research in digital terrain modeling, that cubic spline functions are most appropriate to represent natural geomorphologic shapes (Hugentobler, 2004), the smoothing interpolation was computed with a bi-cubic spline function.

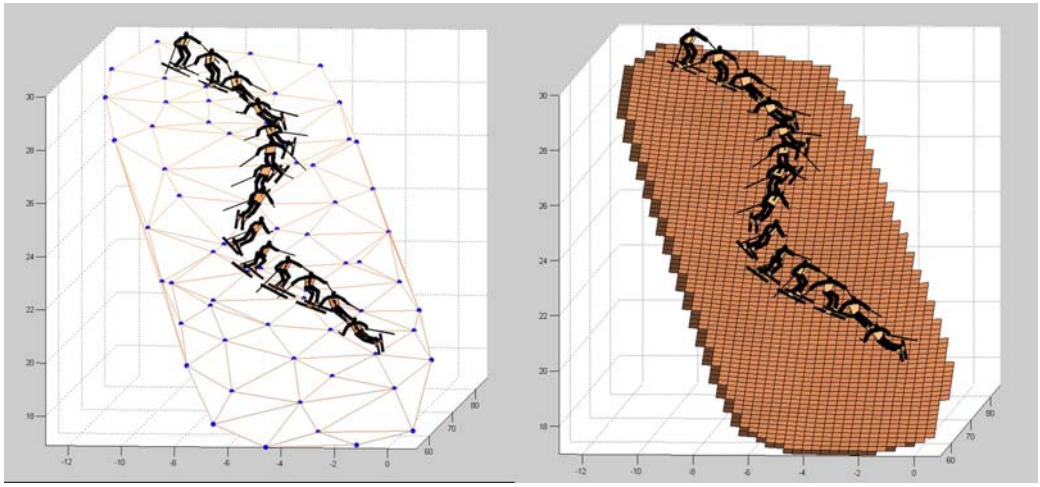

Figure 20: *The comparison of the triangulation based model on the left with the smoothed on the right hand side.*

The bi-cubic spline function was computed on the rectangular grid. The function passes through the captured data points and interpolates the elevation of the surface at the grid points within between. (Watson, 1993; Sandwell, 1987). The differences in terms of loss in degree of model detail between the smoothed model and the two simpler models were computed. The residual difference in normal direction on the least-square plane were 5.7 cm in average and 27.1 maximally (Gilgien et al., 2008). For the triangulation

model the residual differences were 2 cm in average and 7.8 cm maximally. Since the differences in model detail are too small to be visualized the functions applied on the points captured on the snow surface points were run on a very simple pyramid model consisting of 5 points. The figures 21 – 25 visualize the different characteristics of the above discussed models.

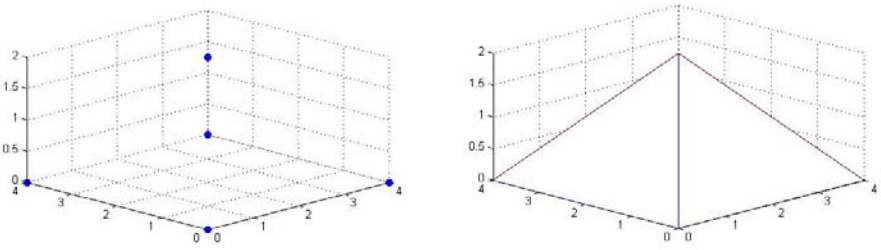

Figure 21: *Five points spanning a pyramid on the left and the triangulation based model on the right-hand side.*

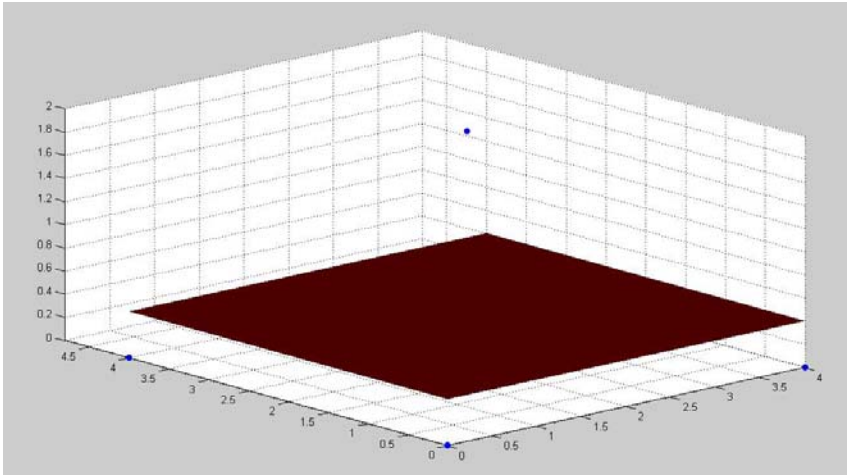

Figure 22: *Least-square plane in red and the edges of the pyramid in blue.*

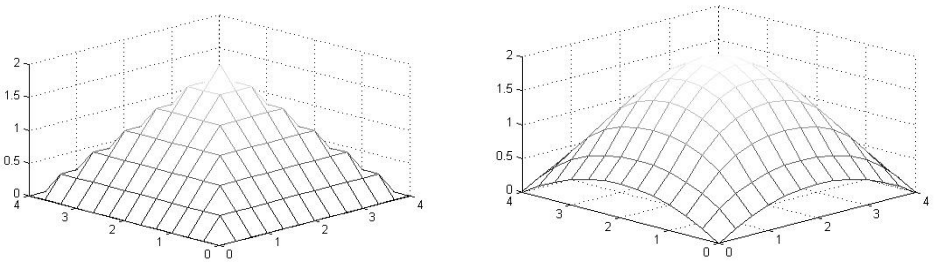

Figure 23: *The same pyramid as above calculated on a rectangular grid data with linear interpolation between the captured points on the left side and a bi-cubic interpolated surface based on the same rectangular grid on the right-hand side.*

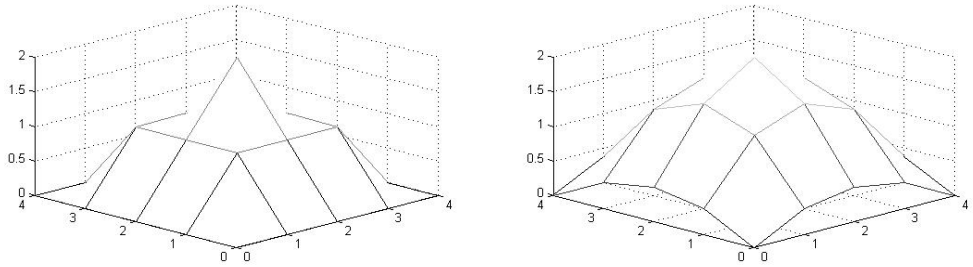

Figure 24: *The same interpolation functions applied on a grid with increased side length causes a rougher representation of the object.*

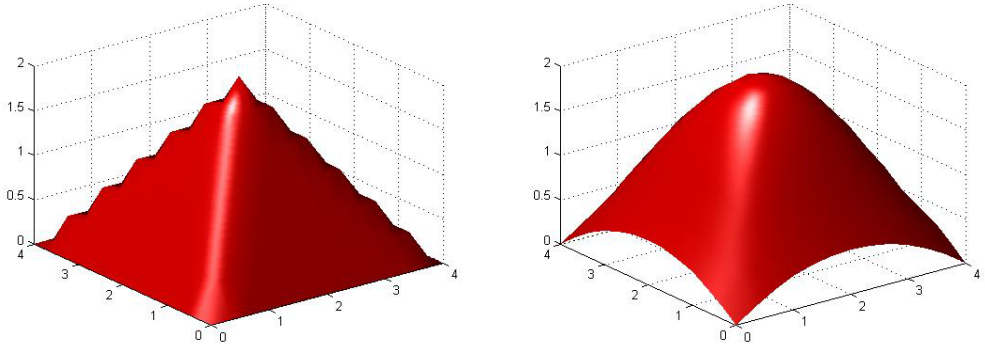

Figure 25: The same procedure applied as in figure 8 but without the grid shown in the representation.

2.16 Derivation of local gradients

By the mean of standard trigonometry local gradients were calculated at the grid points of the smoothed digital terrain model. A visualisation of the local gradients indicated by arrows knotted to the grid with 40 cm side length is shown in figure 26. The perspective of the graph is normal to the snow surface. The red line is indicating the main direction of the course calculated as a regression line between the 4 gates. Figure 27 illustrates the distribution of local gradients pointing in the direction of the average gradient.

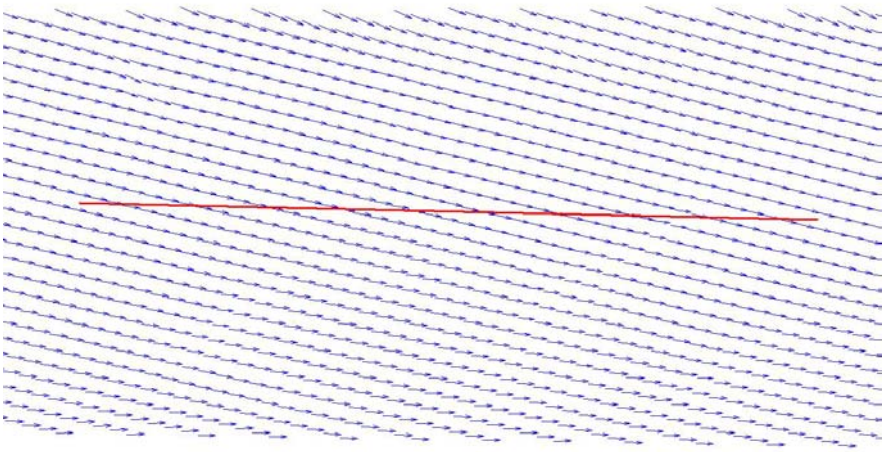

Figure 26: *Local gradients represented by the blue arrows knotted to the grid and the main course direction indicated by the red line.*

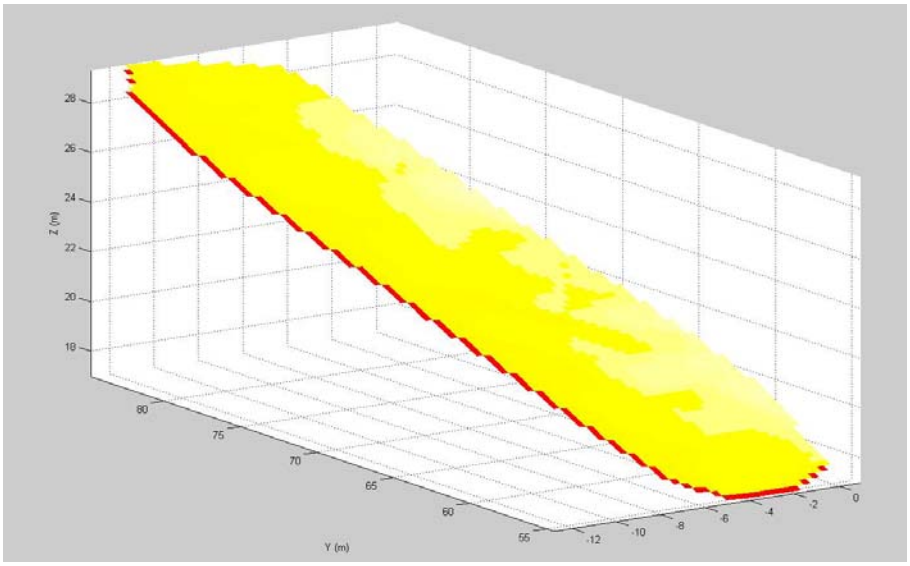

Figure 27: *The snow surface coloured according to the direction of the local gradients. The brighter the yellow the more are the gradients pointing towards the direction we are looking from at the graphics.*

Interestingly, the average angle between the gradients and the main direction of the course of 14.5º was bigger than what we expected from our unaided eye guess during the data collection. A reason for this misjudgement might be that the general inclination was - in geometrical scales speaking - small. If the inclination along the direction of a gradient is small a small deviation in the inclination causes a relative big change in the direction of the angle between them. In case the general inclination is big a small deviation in the inclination causes the angle between the gradients to be small. The illustration below is meant to make this clear.

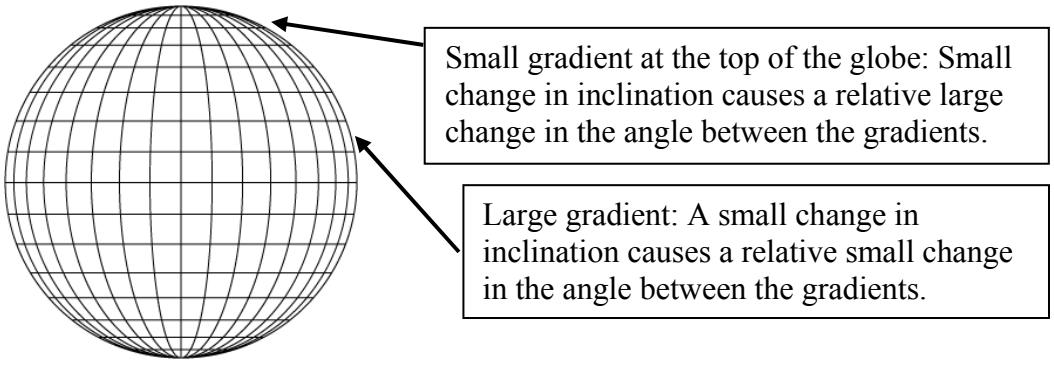

This finding indicates that the direction of the course setting should be based on quantitative measures of the local inclination of the slope in case the minimization of the angle between the main direction of the course and the gradient is an issue in further investigations. This might be an important issue in investigations dealing with the measurement of ground reaction forces and the distribution of ski loading forces between in and outside ski.

2.17 Computation of the COM velocity and acceleration

The instantaneous velocity and acceleration of the COM was calculated by the first and second derivation of the 5 Hz 2nd order Butterworth filtered COM position data. The components acting in the direction of the COM velocity vector were decomposed from $F_{resultant\_total}$ and named $v_{\_COM\_V}$ and $a_{\_COM\_v}$ respectively. For use in model 2, which was based on the projection of the COM on the snow surface and model 3 that's F_{slope} is based on the inclination of the slope at where the skis are in contact with the snowsurface, $v_{\_COM\_V}$ and $a_{\_COM\_V}$ were decomposed by projection into the least-square plane and named $v_{\_COM\_||}$ and $a_{\_COM\_||}$.

2.18 Computation of the external forces acting on the skier in the direction of travel

The derivation of the forces as they are defined in the theory chapter, are described here in more detail. An illustration of the definition of the forces for the different models is given in figure 28 and 29.

Figure 28: *to the left: The external forces acting on the skier and their components in direction of travel. To the right: Definition of* F_{slope_COM} *and* $F_{resultant\_travel}$ *for the force model 1.*

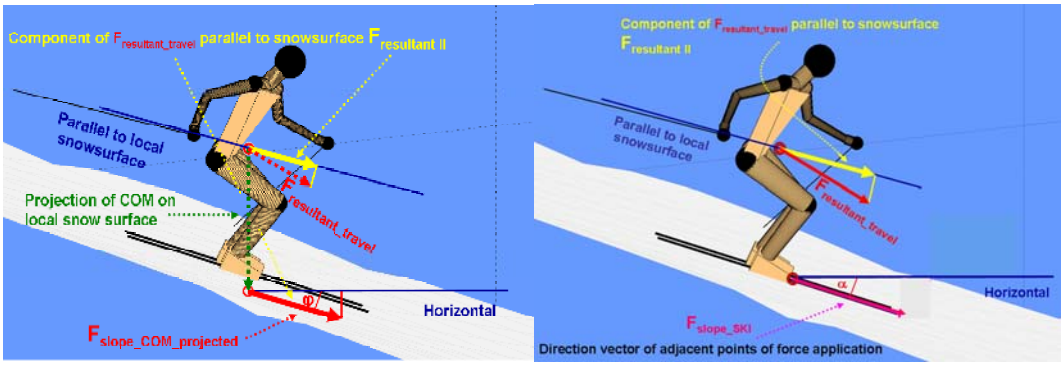

Figure 29: *Left graph: Definition of Fslope_COM_projected and Fresultant_|| for the force model 2. Right graph: Definition of Fslope_SKI and Fresultant_|| for the force model 3*

2.18.1 Computation of the resultant forces acting in the direction of travel

$F_{resultant\_travel}$:

$F_{resultant\_travel}$ is used in model 1. It is derived by the decomposition of the total resultant force into the direction of the velocity vector. The mass of the skier includes the mass of the equipment.

$$F_{resultant\_travel} = a_{COM\_V} \cdot m$$

Equation 4

$F_{resultant\_||}$:

$F_{resultant\_||}$ was computed by the projection of $F_{resultant\_travel}$ into the least-square plane. $F_{resultant\_||}$ excludes the vertical movement in direction normal to the local snow surface.

$$F_{resultant\_||} = a_{COM\_V\_||} \cdot m$$

Equation 5

2.18.2 Computation of the component of gravity pulling the skier downhill

F_{slope_COM}:

F_{slope_COM} is used in model 1 and was derived by decomposition of the vertical component of $F_{resultant\_travel}$.

$F_{slope\_COM\_projected}$:

$F_{slope\_COM\_projected}$ is used in model 2 and derived by the decomposition of the vertical component of $F_{resultant\_||}$.

F_{slope_SKI}:

F_{slope_SKI} is considered dependent on the inclination of the slope at the skiers instantaneous location and the angle the skier is travelling at relative to the gradient. Howe (Howe, 2001) described the direction the skier is travelling at as being the direction of the skis. We disagree with him, since the direction of travel is not along the

direction of the skis in any skidding situation. Alternatively we chose to define the direction of travel as the direction of the vector pointing from the present position of the skier on the slope to his position in the adjacent instant, no matter what the orientation of the skis is. The localization of the skier on the slope is not a one-to-one correspondence, since he spans with the skis a wide area of contact with the ground. The point where the resultant ground reaction force intersects with the snow surface was selected to represent the skier's position on the slope. Since we have not measured any ground reaction forces, we are unable to calculate the location of the point of force application (PFA) on the snow surface from kinetics. Instead we compute an approximation which is based on the findings of studies measuring ground reaction force distributions between in and outside ski and the balance point in the longitudinal direction of the skis. We believe this approach being reasonable for the given study, since the snow surface is very uniform and therefore differences to the true point of intersection between the resultant ground reaction force and the snow surface (PFA) are expected to have small effect on the size of F_{slope}. To determine PFA in the saggittal plane, it was assumed that PFA lies on a line connecting the balance points of the ski under the foot of the skier. This assumption seems reasonable to us, since it is - according to Ron LeMaster (LeMaster, 1999) – the midbody of the ski which turns the skier, while the fore- and rear part of the ski turn the ski. We see from pressure distribution insole measurements, that the resultant of the ground reaction force is oscillating relative to the foot through the course of a turn. This true oscillation can not be accessed by our approximation, but might be in a range which does not cause severe differences in the size of F_{slope}, since the snow surface is quite uniform. A more sophisticated model would help for the understanding in cases the skier is truly unbalanced in the sagittal plane as there is one situation in our data (Figure 30).

Figure 30: *Skier in unbalanced position in sagittal plane.*

An approximation which would better accomplish for such extreme situations could be computed by the intersection of a plane spanned by the tips and tail of the skis with the gravitational vector acting on the centre of mass. In such a model the distance from the plane to the snowsurface could be used to determine where the skis touch the snowsurface. This approach could be even refined by the treatment of the skis as an arm of a leversystem applying the ground reaction force on the skier and the calculation of the external forces acting in vertical and lateral direction. For timeline reasons I did not succeed to implement such algorithms and go with the method drafted firstly, where the P_{GRF} in sagittal plane was defined as being on a line connecting the midpoints of the skis in longitudinal direction. The PFA in the frontal plane was defined as a position on the line connecting the midpoints of the skis which describes the position of PFA in sagittal plane. The position of PFA in coronal plane is where the linear combination

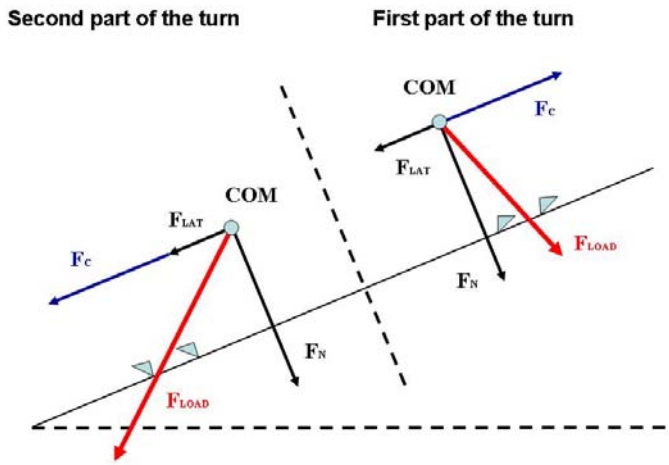

Figure 31: *Vector diagram of the external forces acting in coronal plane. F_{load}: ski loading force; F_C: centrifugal force; F_N and F_{lat}: components of gravity.*

of gravity and the centrifugal force intersects with the snow surface as it is visualized for two situations in figure 31.As long as the skier is in balance in lateral direction the intersection of the resultant force in coronal plane with the snowsurface passes between the inside and outside ski. Our approach to approximate the PFA is based on this fact. Since no ground reaction forces were measured in this study we have applied the pressure distribution between inside and outside ski from other studies in which ski loading was measured (Lüthi et al., 2004; Klous, Müller, & Schwameder, 2008; Müller, Schiefermuller, Kröll, & Schwameder, 2005). Based on their findings the position of the PFA between in and outside ski was computed as an inverse function of the loading.

Concretely, a fraction of the distance between the tips and the tails respectively was determined dependent on the inversely weighted loading of the in and outside skis (Figure 32).

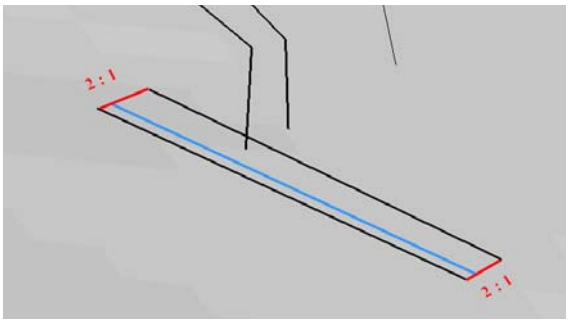

Figure 32: *Ski loading distribution between out- and inside ski of 2:1. In blue the line on which PFA lies in the coronal plane.*

The alteration of the pressure distribution throughout a turn cycle was simulated. In the moment of transition between two turns the loading distribution between in- and outside ski was assumed being 1:1. The transition between two turns was defined as the point where the arithmetic mean of the tips and tails of the skis cross the trajectory of the COM when they are projected into a plane parallel to the local snow surface (Supej, Kugovnik, & Nemec, 2003). We have further defined the beginning of the turn as where the COM turn radius drops below 15m and the turn end as where the COM turn radius goes beyond 15m. The loading of the outside ski increases gradually from 1:1 at the switch to 2:1 at the beginning of the turn and stays constant at 2:1 until the end of the turn. From the end of the turn until the switch the ratio decreases gradually from 2:1 to 1:1 as it is visualized in the graph below. Figure 33 is an visualisation of this algorithm.

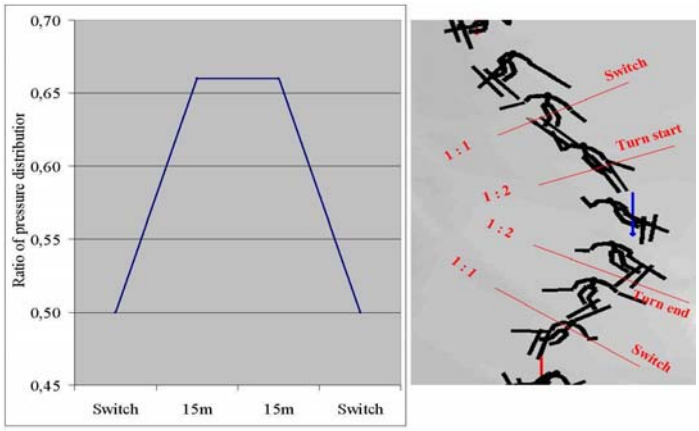

Figure 33: *Ratio of pressure distribution between in- and outside ski for an outside ski throughout a turn.*

The PFA and though the position of the skier on the slope is finally given at where the line connecting the balance points of the skis intersects with the line defining the pressure distribution between in and outside ski.

Due to snow dash's covering parts of the skis, the accuracy of the ski position determination process might be reduced in some situations. We have therefore projected *PFA* normal on the snow surface to make sure the local geomorphology of the slope determines F_{slop_SKIe}. Since the smoothed snow surface consists of 7412 surfaces a memory consuming algorithm was necessary to find the corresponding surface onto which the *PFA* was projected by the means of standard vector geometry Figure 34.

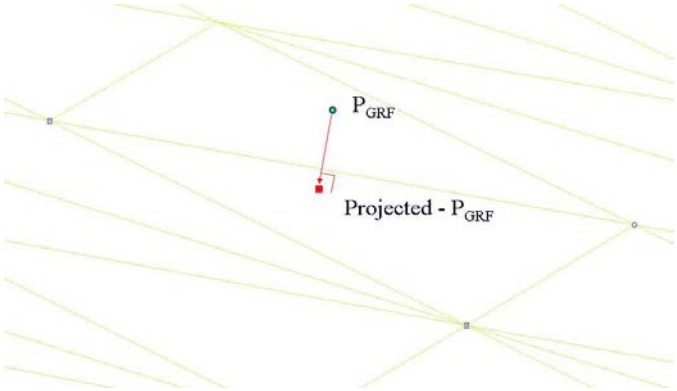

Figure 34: *Projection of the PFA onto the snowsurface.*

Finally, F_{slope_SKI} was computed by the vector between two adjacent projected *PFA as shown in figure 35 and 36.*

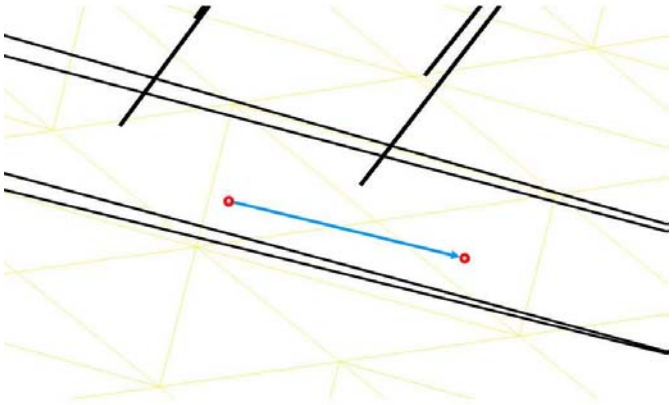

Figure 35: *The vector between two adjacent projected PFA.*

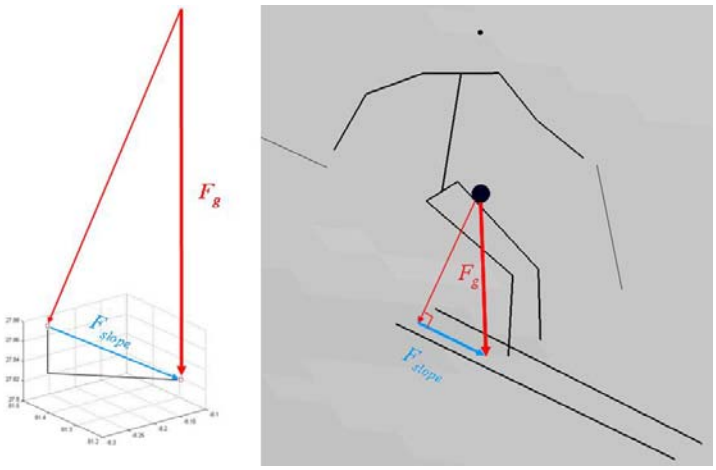

Figure 36: *Illustration of the derivation of F_{slope_SKI} from two adjacent projected PFA.*

2.18.3 Calculation of the wind drag force

The literature dealing with wind drag in alpine skiing is focused on the speed disciplines, since the importance of the wind drag force increases with velocity (Kaps et al., 2005; Luethi & Denoth, 1987; Barelle, Ruby, & Tavernier, 2004; Savolainen, 1989; Candau, Tavernier, Aubail, & Lacour, 1993; Tavernier, Cosserat, Joumard, & Bally, 1994; Kaps et al., 1996). Some investigation had a pure modelling approach (Savolainen, 1989; Candau et al., 1993), others had an experimental setup on the hill (Kaps et al., 2005; Kaps et al., 1996) or wind tunnel testing as basis for their study (Barelle et al., 2004; Luethi et al., 1987; Tavernier et al., 1994). Since the drag force (F_{drag}) acting on a skier is a complex mechanism, we have considered using wind tunnel testing or advanced computational fluid dynamics to compute F_{drag}. We dropped these ideas, when we understood, that such an analyses would represent a work volume of a Masters degree for its own. This choice was encouraged by the finding that the size of F_{drag} is of minor size relative to the frictional force acting in the ski-snow interaction in slalom. Therefore would a relative big error in the determination of F_{drag} have a small effect on the total braking force. The estimation of the relative size of $F_{drag}$was based on the extrapolation of regression analysis models describing the external forces in standard situations. We used parameters from the literature dealing with alpine (Barelle et al., 2004; Luethi et al., 1987) and cross country skiing (Spring, Savolainen, Erikkila, Hamalainen, & Pihkala, 1988b), varied the factors which have effect on F_{drag} in the model and could conclude that the size of the variability of F_{drag} was small compared to the other external forces acting on the skier in the direction of travel.

We have therefore chosen to compute the estimation of the wind drag forces based on a simple model taking in account the frontal area exposed to the wind (A), the velocity (v), the air density ρ, an estimate of the drag coefficient (c_d). The drag coefficient c_d describes the frictional properties in the boundary layer along the skier's surface as well as the drag properties due to the skiers shape. A lifting component was not addressed, since only forces in direction of travel are of interest in this study. The wind velocity was assumed being 1m/s flowing against the skier's travel direction. At the spot no wind measurements were taken, but the meteorological station at Gardermoen reported average wind velocities of 3m/s at 6 o'clock in the morning.

$$F_{drag} = c_d \cdot \frac{\rho \cdot v^2}{2} \cdot A$$

Equation 6

This equation is valid for Reynolds numbers > 1000.

Calculation of the drag coefficient

The choice of the drag coefficient *(c_d)* is probably the most uncertain factor in this estimation, since its value was never measured in wind tunnel testing for alpine skiers at characteristic speed in slalom. It needs therefore to be adapted from measurements in other sports.

Older studies investigating air drag in alpine skiing were mistaken by posting that c_d is independent of velocity (Habel, 1968; Leino & Spring, 1984). This view was later corrected (Spring, Savolainen, Erikkila, Hamalainen, & Pihkala, 1988c; van Ingen Schenau, 1982b; Tavernier et al., 1994; Kaps et al., 2005) and it is now a well established fact, that c_d varies with velocity. One study (Gorlin, Maseev, Zyrjanov, & Remizov, 1987) could show, that the drag coefficient for skiers was about halved when velocity was increased from 10 to 15 m/s and about constant in the range from 15 to 45 m/s but was not quantified in true absolute size. The drop of c_d in that range of speed was confirmed on request by Luca Oggiano, working with wind tunnel testing in sports at NTNU in Trondheim (Oggiano, 2007).

"*There is actually a transition and I'm quite sure that for downhill skiing this transition should happen around 16m/s. In speed skating the fall in Cd happens already at 10-12m/s. This is due to the golf ball textiles used on the legs."*

The range of velocities in our study reaches from 11 to 13 m/s (Haugen et al., 2007) and we are therefore most probable in the transition area where c_d is strongly dependent on the velocity.

To understand why the drag coefficient is dependent on velocity, we have to go into the mechanisms of fluid dynamics. The total drag force on an object is dependent on both friction drag and pressure- or inertial drag. Friction drag occurs due to frictional forces in the boundary layer of the air. Pressure- or inertial drag occurs due to the pressure difference from the luff- to the leeside of a body. As a standard measure of the relative contribution of the two types of drag to the total F_{drag} the ratio of inertial to frictional drag is called the Reynolds number. The Reynolds number (Re) is a dimensionless number and calculated as shown below.

$$\mathrm{Re} = \frac{\mathrm{inertialforce}}{\mathrm{frictionalforce}} = \frac{\frac{\rho \cdot v^2}{l}}{\frac{\eta \cdot v}{l^2}}$$

Equation 7

v is the instantaneous relative velocity in the direction of travel between the body and the airflow. l is a characteristic length of the body exposed to the airflow. In our field of study this might be the diameter of the trunk and in fundamental fluid dynamics research the diameter of a sphere for example. ρ is the density of the air.

Simplification of the equation describing the Reynolds number leads to a form, where Re is dependent on velocity *(υ)*, the characteristic length *(l)* of the object and the kinetic viscosity *(v)* only. Based on this relation the Reynolds number and processes in fluid dynamics of simple objects were studied in detail AA and are well understood. The understanding of the process in simple objects can help us to get to a better understanding of the underlying processes in more complex bodies, such as the human

body, since the human body can to some degree be treated as a composition of cylinders. Figure 37 illustrates the flow of a fluid around a cylinder.

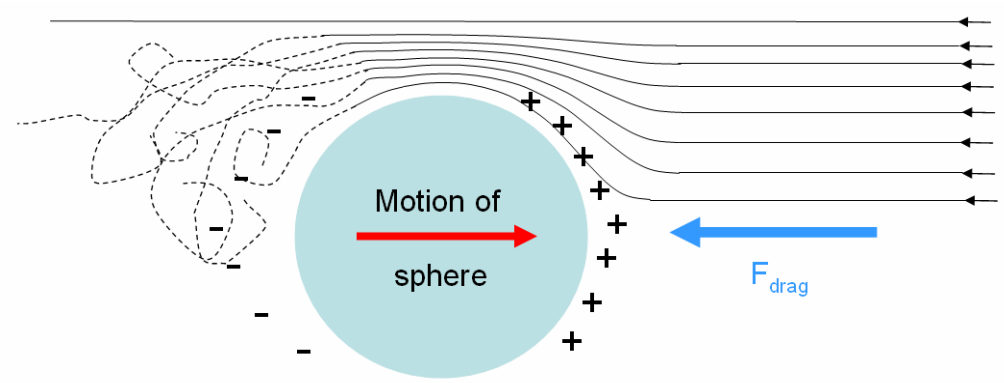

Figure 37: *Airflow around a cylinder, with the high pressure area on the front side of the cylinder, the low pressure area and turbulence on the downstream side of the cylinder.*

If the velocity of the airflow is very low (or the velocity of the object relative to the ambient air), friction drag can be dominant in size over pressure drag and the Reynolds number is therefore below 1. In such a situation Stokes' law rules and c_d is inversely proportional to the velocity and therefore F_{drag} is proportional to the velocity. If the Reynolds number increases up to 1000, indicating, that the inertial drag component becomes more and more important than the frictional component, the difference in velocity from the luff- to the lee side of the object increases. On the front side of the object the airflow velocity is close to zero (stagnation point) while the air gets accelerated when flowing around the body. This velocity difference causes a high pressure area in front and a turbulent low pressure area object. Due to the high velocities the fluid is separating from the object at a position moving towards the frontal side of the body with increasing velocity. If the Reynolds number is between 10^3 and 10^5 the total drag force is about constant because the separation of the boundary layer from the surface occurs at the same location. If Re is beyond 10^5 the F_{Drag} is decreased due to turbulences in the boundary layer itself, which causes the boundary layer to separate from the surface (separation point) more on the leeside of the object.

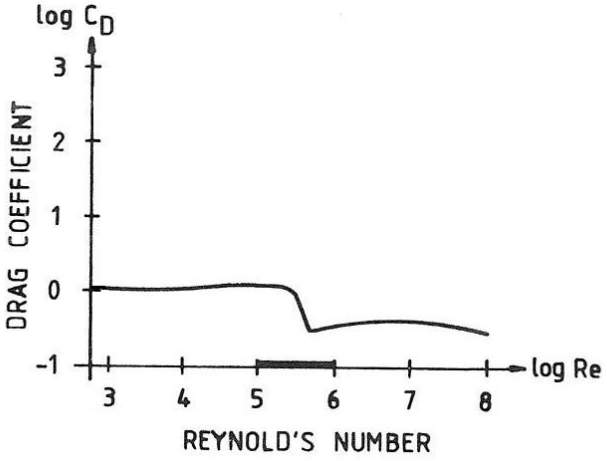

***Figure 38**: Dependency of the drag coefficient c_d on the Reynolds number, Re for a cylinder with the rapide change of c_d between10^5 and10^5. From: " Drag area of a crosscountry skier ." By: Spring, E., Savolainen, S., Erikkila, T., Hamalainen, T., & Pihkala, P. ,1988, International Journal of Sport Biomechanics, 4, 106. Copyright by Human kinetics Inc. 1988.*

The rapid change in c_d for Re between 10^5 and 10^6 (figure 38) was described to occur between 0 and 17 m/s (Kaps et al., 1996)and between 10 and 15 m/s (Gorlin et al., 1987). The body shape and positioning has effect on c_d as well (Kaps et al., 1996), since the simplification by describing the size and shape of the human body by a composition of cylinders or a characteristic length *l* has its limitations. Some studies have therefore chosen to describe the drag area ($c_d \cdot A$) as a function of knee and hip angles (van Ingen Schenau, 1982a; Barelle et al., 2004) or a function of body extension (Barelle et al., 2004; Spring, Savolainen, Erikkila, Hamalainen, & Pihkala, 1988a). The model of Barelle et al. (2004) is based on wind tunnel testing and the drag area ($c_d \cdot A$) is computed as a function of body posture of the skier. Specifically, the length of segments and the angles of trunk- and segmentpostures are given as functions of c_d. The model was unfortunately validated for speed disciplines equipment and velocities above 14 m/s only and the uncertainty around ($c_d \cdot A$) is therefore too big to be implemented in our study. Instead we have computed frontal area and implemented c_d values derived from a paper dealing with wind drag in crosscountry skiing (Spring et al., 1988a). Spring et at. have computed the drag area ($c_d \cdot A$) of male cross-country skiers as a function of their velocity for an uprised and a crouched posture in the velocity range of 5 to 12 m/s (figure 39). Since they have measured the projected frontal area we could access the

respective drag coefficient for the two postures by dividing the drag area by the frontal area; $c_d = (c_d \cdot A)/A$.

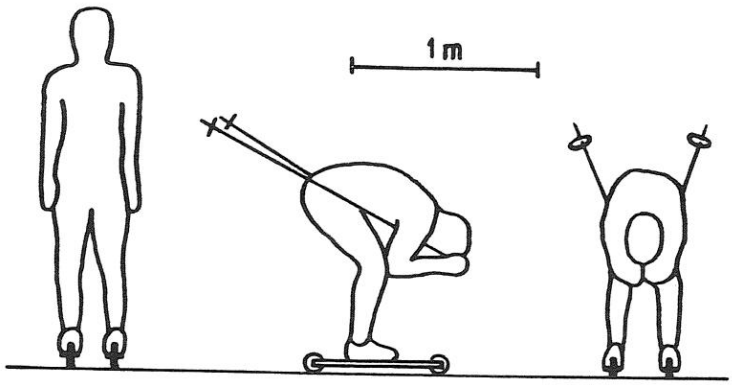

Figure 39: *The up-rised and crouched postures investigated in the study of Spring et al.. From: " Drag area of a crosscountry skier ." By: Spring, E., Savolainen, S., Erikkila, T., Hamalainen, T., & Pihkala, P. ,1988, International Journal of Sport Biomechanics, 4, 108. Copyright by human kinetics Inc. 1988.*

Table 2: *Anthropometric data, projected area and drag area measured for the three skiers From "Drag area of a crosscountry skier ." By: Spring, E., Savolainen, S., Erikkila, T., Hamalainen, T., & Pihkala, P. , 1988, International Journal of Sport Biomechanics, 4, 111. Copyright by human kinetics Inc. 1988.*

Body Dimensions of the Three Skiers

Posture	Skier A	Skier B	Skier C
Upright Posture			
Weight (kg)	80	65	75
Height (m)	1.75	1.65	1.72
Projected area (m^2)	0.65 ± 0.03	0.55 ± 0.03	0.70 ± 0.03
Drag area (m^2)	0.65 ± 0.05	0.56 ± 0.05	0.73 ± 0.04
Semisquatting Posture			
Projected area (m^2)	0.45 ± 0.02	0.38 ± 0.02	0.40 ± 0.02
Drag area (m^2)	0.27 ± 0.03	0.30 ± 0.04	0.33 ± 0.03

One of the skiers wore a sweater and trousers while skier A and B wore tight fitting skiing suits. Their anthropometric measures, the projected frontal area and the drag area are given in Table 2. Since skier A wore a tight fitting skiing suit similar to the one the skiers in our study wore and had anthropometric data much alike the ones of the skiers in our study, we have chosen to use his data to calculate a regression equation which computes the c_d as a function of vertical posture. The c_d for an upright position was

calculated by dividing the drag area by the projected frontal area with the values from the table above. This resulted for the uprised posture with a c_d of $0.65m^2/0.65m^2 = 1.0$ and the semi-squatted posture with $0.27\ m^2 / 0.45m^2 = 0.6$. Imitations of the semi-squatted posture lead us to the assumption that the vertical height above ground would be 1.10m. Based on the vertical height of the silhouettes and the drag coefficients for the two postures a regression equation was computed to give c_c as a function of silhouette height.

Computation of frontal area

The frontal area computation was based on the projection of the silhouette of the skier into a plane normal to the velocity vector of the COM and a pixel counting function (Brodie, 2008). The algorithm was developed to reduce the modeled wind drag errors associated with changing cross sectional area identified as a potential issue in previous work (Brodie, Walmsley, & Page, 2008). The skier's silhouette was built by attaching volumes on the joint centre based line model as illustrated in figure 40. Arm and leg segments were modelled by attaching cones, the shoulder, hip and the neck by attaching cylinders. Hands and joints were represented by spheres and the head by an ellipsoid. Shoes were constructed by a composition of parallelepipeds and cuboids. The boundary lines of the trunk body were based on systematic offsets of the hip and shoulder joints.

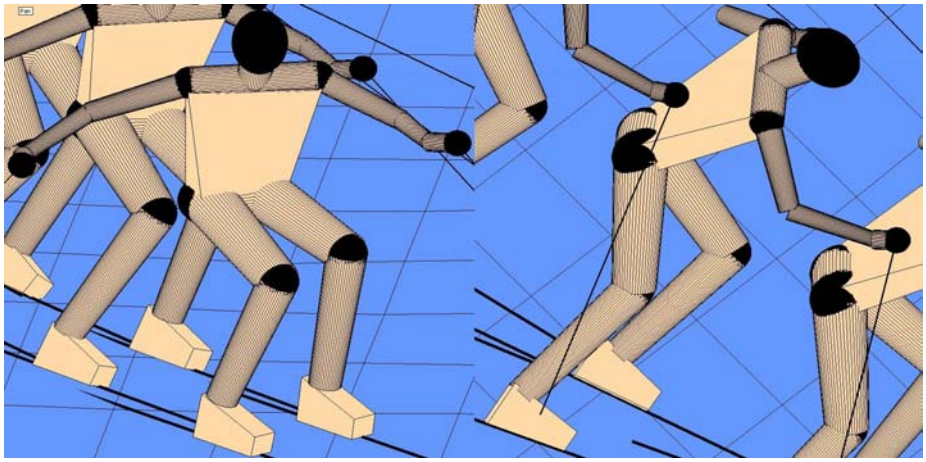

***Figure 40**: Skier model with volumes attached to the lines which connect joint centers.*

To avoid distortion in the projection of the frontal area into the plane normal to the COM velocity vector we used an orthographic projection. The area within the silhouette of the projected skier was coloured white and the background black. The pixel counting

function computed the white coloured pixels and the area within a square spanning $1m^2$ as illustrated in figure 41. The number of pixels within the square was used to calibrate the pixels representing the frontal area of the skier to an area given in m^2.

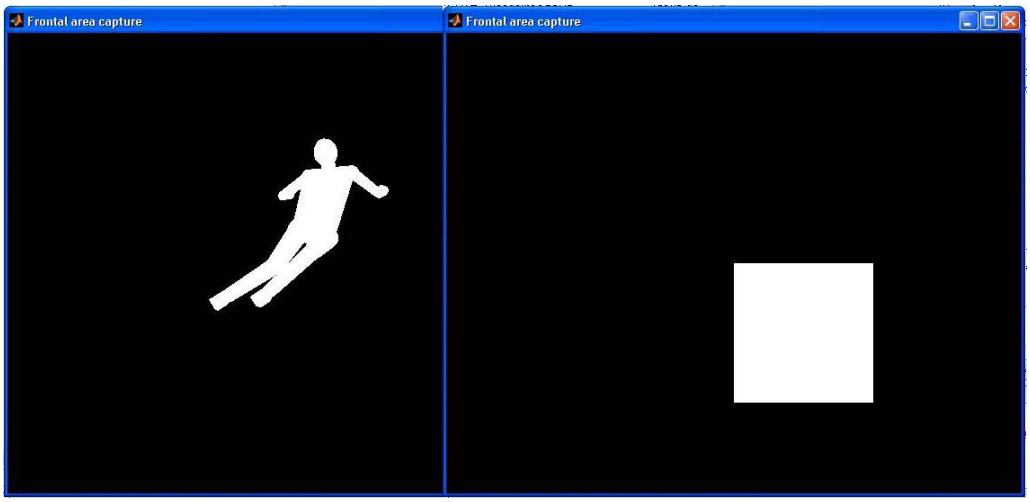

***Figure 41**: MalLab frames with the coloured silhouette of the skier on the left and the calibration square on the right side.*

Calculation of air density

The density of air ρ was calculated from temperature measurements which were taken during the measurements at the area of investigation and the air pressure taken at the meteorological station which is placed 18km in north-east direction at Gardermoen airport. For dry air ρ is dependent on the air pressure (p) and the temperature (*T*). *R* is the specific gas constant.

$$\rho = \frac{p}{R \cdot T}$$

Equation 8

For humid air the air pressure decreases with increasing humidity, since the molecular mass of water is smaller than the molecular mass of air. The air pressure of humid air is composed of the partial pressures of the humid and dry air with their specific gas constants. In this investigation the influence of air humidity was neglected, being less than 2% (van Ingen Schenau, 1982a).

Wind velocity and direction

At 6h in the morning 3.1m/s wind were measured at the meteorological station in Gardermoen coming from direction 150º or south-south-east. Due to the lack of wind measurements we have assumed the following: Since the weather was good a constant wind from the valley, a so called valley wind, in uphill direction is to be expected. Valley winds occur during daytime in high pressure weather situations as it was the case on the day the investigation was conducted. They originate in a convective compensation flow due to intense radiation usually starting in the morning and lasting until the afternoon. Due to the snow covering the flanks of the valley, the compensation flow can not be expected to be as strong as in snow free conditions, when more radiation is absorbed by the ground (Malberg, 2002). The 3.1m/s wind from SSE are assumed to be present during the data collection as a large-scale circulation. The angle to the main direction the skiers were travelling at is about 120º, but a ridge on the south-east side of the slope (figure 42) might cause the wind streaming from about 90º to the mean direction of travel and might therefore only have slight effect in the end of right turns. The valley wind, a small range terrain meteorological phenomena, might be flowing in opposite direction the skiers were skiing at and is assumed to be 1 m/s since the observers did not register well appreciable wind (Malberg, 2002).

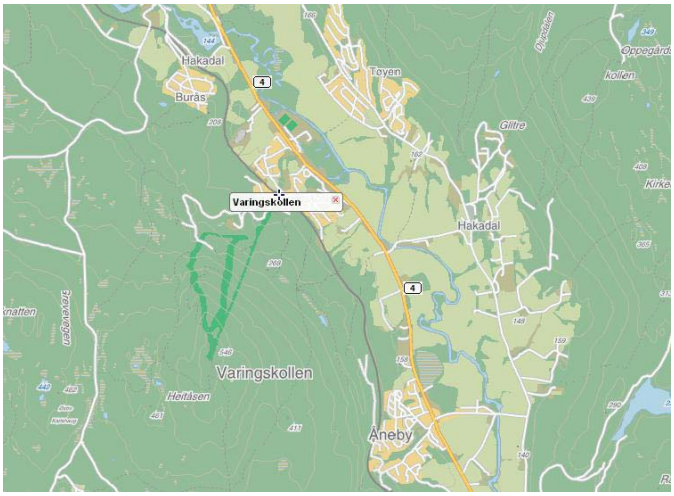

Figure 42: *The skiingarea Varingskollen and its surroundings. The valley ranging in north-west to south-east direction and the flanks on both sides.*

Calculation of the relative velocity

The velocity the wind and the skier were moving relative to each other was computed by adding the instantaneous velocity of the COM and the assumed wind stream of 1m/s in the opposite direction to the skier's direction of travel.

2.18.4 Frictional force

The braking force due to friction between ski and snow and the packing of the snow is calculated from the difference equation. For the different models the respective forces are named as given below.

Model 1:

$$F_{friction\_1} = F_{slope\_COM} - F_{resultant\_travel} - F_{drag}$$

Equation 9

Model 2:

$$F_{friction\_2} = F_{slope\_COM\_projected} - F_{resultant\_||} - F_{drag}$$

Equation 10

Model 3:

$$F_{friction\_3} = F_{slope\_SKI} - F_{resultant\_||} - F_{drag}$$

Equation 11

2.19 Energy dissipation

For the calculation of E_{diss} the 2nd order Butterworth 5 Hz filtered data were used and calculated central finite central differences.

$$\begin{aligned} ME &= PE + KE \quad [J] \\ &= mgh + \frac{1}{2}mv^2 \quad [J] \\ E_{diss} &= \frac{\Delta ME}{m\Delta h} \quad [J \cdot kg^{-1} \cdot m^{-1}] \end{aligned}$$

Equation 12

(Supej et al., 2005) originally changed the sign of the right-hand side of the equation describing E_{diss}, to make energy dissipation easier to understand for coaches and

athletes. We have not chosen to do such an adjustment to stay in line with its definition. Positive energy dissipation indicates the loss of energy to the surrounding and, conversely, negative dissipation represents the gain of energy due to the athlete's muscular work. In the visualisation of the data we choose to draw energy dissipation with the opposite sign, but do not adjust its definition as Supej did.

2.20 Key movement characteristics occurring during periods when energy dissipation is negative

The quantification of movement characteristics potentially producing propulsion was based on three measures: The angle between the instantaneous velocity vector of *PFA* and the COM velocity vector, both projected in the least-square-plane, was computed as a measure for skating-like movements. The distance of the COM normal to the local snow surface was computed as a measure for the vertical movement. The quantification of the fore/aft movement of the skis relative to the COM was based on the distance spanned by the PFA and its projection into the plane normal to $v_{\_COM\_||}$.

2.21 Definition of the turn transition

According to separate two turns from each other the transition was defined as the point where the trajectory of the arithmetic mean position of the tips and tails of the skis cross the COM trajectory in the plane parallel to the snow surface (Supej et al., 2003).

2.22 Time normalization

Data were time-normalized as a percentage of the total turn cycle. Descriptive statistics and ensemble averages were calculated for each parameter using six athletes on two turns.

3. References

Reference List

Abdel-Aziz, Y. I. & Karara, H. M. (1971). *Direct linear transformation from comparator coordinates into object space coordinates in close-range photogrammetry.* In *Symposium on Close-Range Photogrammetry* (pp. 1-18). Falls Church: American Society of Photogrammetry.

Barelle, C., Ruby, A., & Tavernier, M. (2004). *Experimental Model of the Aerodynamic Drag Coefficient in Alpine Skiing. Journal of Applied Biomechanics, 20,* 167-176.

Brodie, M. (28-10-2008). *Pixel counting algorithm to estimate wind drag.* Ref Type: Personal Communication

Brodie, M., Walmsley, A., & Page, W. (2008). *Fusion Motion Capture:* A Prototype System Using IMUs and GPS for the Biomechanical Analysis of Alpine Ski Racing. *Journal of Sports Technology, 1,* 17-28.

Candau, R., Tavernier, M., Aubail, R., & Lacour, J. R. (1993). *Relationships between performance, aerodynamic resistance, ski-snow friction resistance, and anatomic characteristics of lower limbs in 12 elite alpine skiers.* In *International Society of Biomechanics XIVth Congress* (pp. 234).

Chalmers, A. F. & Lyngs, G. (1995). *Hvad er videnskab?: En indføring i moderne videnskabsteori.* Copenhagen: Gyldendal.

Chen, L., Armstrong, C. W., & Raftopoulos, D. D. (1994). *An investigation on the accuracy of three-dimensional space reconstruction using the direct linear transformation technique. Journal of Biomechanics, 27,* 493-500.

de Berg, M., Otfried, C., van Kreveld, M., & Overmars, M. (2008). *Computational Geometry: Algorithms and Applications*.

de Leva, P. (1996). *Adjustments to zatsiorsky-seluyanov's segment inertia parameters. Journal of Biomechanics, 29,* 1223-1230.

Ducret, S., Ribot, P., Vargiolu, R., Lawrence, J., & Midol, A. (2004). *Analysis of Downhill Ski Performance Using GPS and Ground Force Recording.* In D. Bacharach & J. Seifert (Eds.), *3rd International Congress on Skiing and Science* St. Cloud State University.

Gilgien, M., Reid, R., Haugen, P., & Smith, G. (2008). *Digital terrain modelling of snow surfaces for use in biomechanical investigations in snow sports.* In *13th Annual Congress of the European College of Sport Science*.

Gilgien, M., Reid, R., Tjørhom, H., Moger, T., Haugen, P., Kipp, R. et al. (2007). *Energy dissipation and slalom turn radius.* In *4th International Congress on Science and Skiing 2007* Salzburg, Austria: E. Müller, S. Lindinger, T. Stöggl, & V. Fastenbauer.

Gorlin, M., Maseev, W., Zyrjanov, W., & Remizov, L. (1987). *Sliding friction and boundary lubrication of snow. Journal of Tribology, 109,* 614-617.

Habel, B. (1968). *Über die Bestimmung von Luftwiderstand und Gleitreibung beim Skilauf. Europa Sport, 20,* 950-955.

Haugen, P., Reid, R., Tjørhom, H., Moger, T., Gilgien, M., Kipp, R. et al. (2007). *Centre of mass velocity and the turn cycle in slalom.* In *4th International Congress on Science in Skiing*.

Howe, H. (2001). *The New Skiing Mechanics*.

Hugentobler, M. (2004). *Terrain Modelling with Triangle Based Free-Form Surfaces.* ETH Zurich, Switzerland.

Kaps, P., Nachbauer, W., & Mossner, M. (2005). *Snow friction and drag in alpine downhill racing.*
Ref Type: Unpublished Work

Kaps, P., Nachbauer, W., & Mossner, M. (1996). *Determination of kinetic friction and drag area in alpine skiing.* In C.D.Mote, R. J. Johnson, W. Hauser, & P. S. Schaff (Eds.), *Ski Trauma and Skiing Safety: 10th Volume* (Philadelphia: American Society for Testing and Materials.

Klous, M., Müller, E., & Schwameder, H. (2008). *Knee joint loading an alpine skiing: A comparison between carved and skikked turns.* In *12th Annual Congress of the European College of Sport Science*.

Leino, M. & Spring, E. (1984). *Determination of the coefficient of kinetic friction between ski and snow from gliding velocity of a skier. Geophysics, 19*.

LeMaster, R. (1999). *The skiers edge*. Human Kinetics.

Lind, D. & Sanders, S. (2003). *The Physics of skiing*. (2nd ed.) New York: Springer.

Luethi, S. & Denoth, J. (1987). *The Influence of Aerodynamic and Anthropometric Factors on Speed in Skiing. International Journal of Sport Biomechanics, 3,* 345-352.

Lüthi, A., Federolf, P., Fauve, M., Oberhofer, K., Rhyner, H., Amman, W. et al. (2004). *Determination of forces in carving using three independent methods.* In D. Bacharach & J. Seifert (Eds.), *3rd International Congress on Skiing and Science* (pp. 3-4). St. Cloud State University.

Malberg, H. (2002). *Meteorologie und Klimatologie: Eine Einführung*. Springer.

Moger, T., Reid, R., Haugen, P., Tjørhom, H., Gilgien, M., & Smith, G. (2007). *Kan en ved hjelp av en 3 dimensjonal kinematisk analyse beskrive tyngdepunktsbanen til SL - løpere nøyaktig nok til å beskrive viktige prestasjonskarakteristika til tyngepunktsbanen?* Norwegian School for Sport Science, Oslo, Norway.

Mossner, M., Kaps, P., & Nachbauer, W. (1996). *A method for obtaining 3-d data in alpine skiing using pan-and-tilt cameras with zoom lenses.* In C.D.Mote, R. J. Johnson, W. Hauser, & P. S. Schaff (Eds.), *Skiing Trauma and Safety: Tenth Volume* (pp. 155-164). Philadelphia: American Society for Testing and Materials.

Müller, E., Schiefermuller, C., Kröll, J., & Schwameder, H. (2005). *Skiing with carving skis - what is new?* In E.Müller, D. Bacharach, R. Klika, S. Lindinger, & H. Schwameder (Eds.), *3rd International Congress on Skiing and Science* (pp. 15-23). Oxford: Meyer & Meyer Sport.

Nachbauer, W., Kaps, P., Nigg, B., Brunner, F., Lutz, A., Obkircher, G. et al. (1996). *A video technique for obtaining 3-d coordinates in alpine skiing*. *Journal of Applied Biomechanics, 12,* 104-115.

Oggiano, L. (12-12-2007). *Drop of cd at Reynolds numbers between 10^5 and 10^6.* Ref Type: Personal Communication

Pourcelot, P., Audigie, F., Degueurce, C., Geiger, D., & Denoix, J. M. (2000). *A method to synchronize cameras using the direct linear transformation technique*. *Journal of Biomechanics, 33,* 1751-1754.

Reid, R., Gilgien, M., Moger, T., Tjørhom, H., Haugen, P., Kipp, R. et al. (2008). *Turn characteristics and energy dissipation in slalom*. In *4th International Congress on Science and Skiing 2007* Salzburg, Austria: E. Müller, S. Lindinger, T. Stöggl, & V. Fastenbauer.

Reid, R., Tjørhom, H., Moger, T., Haugen, P., Kipp, R., & Smith, G. (2007). *Accuracy od 3d position prediction over a large object space using pan and tilt cameras*. In *12th Annual Congress of the European College of Sport Science*.

Sandwell, T. (1987). *Biharmonic Spline Interpolation of GEOS-3 and SEASAT Altimeter Data. Geophysical research letters, 14,* 139-142.

Savolainen, S. (1989). *Theoretical Drag Analysis of a Skier in the Downhill Speed* Race. *International Journal of Sport Biomechanics, 5,* 26-39.

Schiestl, M. (2005). *Improving DLT precision with constant camera parameters.* Ref Type: Unpublished Work

Schiestl, M., Kaps, P., Mossner, M., & Nachbauer, W. (2005). *Snow friction and drag during the downhill race in Kitzbuhel.* In *Mountain and sport: Updating study and research from laboratory to field* (pp. 54).

Schiestl, M., Kaps, P., Mossner, M., & Nachbauer, W. (2006). *Calculation of friction and reaction forces during an alpine world cup downhill race*. In E.F.Moritz & S. Haake (Eds.), *The engineering of sport 6, Volume 1: Developments for sports* (pp. 269-274). New York: Springer.

Shapiro, R. (1978). *Direct linear transformation method for three-dimensional cinematography. Research Quarterly, 49,* 197-205.

Spring, E., Savolainen, S., Erikkila, T., Hamalainen, T., & Pihkala, P. (1988a). *Drag area of a crosscountry skier*. *International Journal of Sport Biomechanics, 4,* 103-113.

Supej, M. (2003). *The myth of acceleration and push-off in racing alpine skiing.* Ref Type: Unpublished Work

Supej, M. (2008). Differential specific mechanical energy as a quality parameter in racing alpine skiing. *Journal of Applied Biomechanics*.

Supej, M., Kugovnik, O., & Nemec, B. (2005). *Energy principle used for estimating the quality of a racing ski turn.* In E. Müller, D. Bacharach, S. Klika, S. Lindinger, & H. Schwameder (Eds.), *3rd international congress on science in skiing* (pp. 228-237). Adelaide: Meyer & Meyer Sport Ltd..

Supej, M., Kugovnik, O., & Nemec, B. (2003). *Kinematic determination of the beginning of a ski turn. Kinesiologia Slovenica, 9,* 11-17.

Supej, M., Kugovnik, O., & Nemec, B. (2004). *The energy principle used for estimating the quality of the racing ski turn.* In D. Bacharach & J. Seifert (Eds.), *3rd International Congress on Skiing and Science* (pp. 63-64). St. Cloud State University.

Tavernier, M., Cosserat, E., Joumard, E., & Bally, P. (1994). *Influences des effets aérodynamiques et des appuis ski-neige sur la performance en ski alpin. Science et motricité,* 21-26.

Tjørhom, H., Reid, R., Haugen, P., Moger, T., Gilgien, M., & Smith, G. (2007). *Beskrivelse av tyngdepunktets frem/bak dynamikk i slalåm sett opp mot prestasjon ved hjelp av en 3 dimensjonal kinematisk analyse.* Norwegian School for Sport Science, Oslo, Norway.

van Ingen Schenau, G. J. (1982a). *The inuence of air friction in speed skating*. *Journal of Biomechanics, 15,* 449-458.

Watson, D. F. (1993). *Contouring: a guide to the analysis and display of spatial data. Computers & Geosciences, 19,* 1389-1391.

Wood, G. A. & Marshall, R. N. (1986). *The accuracy of dlt extrapolation in three-dimensional film analysis*. *Journal of Biomechanics, 19,* 781-785.

Zatsiorsky, V. M. (2002). *Kinetics of human motion*. Champaign: Human Kinetics, Inc.

Zatsiorsky, V. M. & Seluyanov, V. (1985). *Estimation of the mass and intertia characteristics of the human body by means of the best predictive regression equations*.

4. Scientific paper

Abstract

The share of literature describing the kinetics of alpine skiing is limited in general, but especially in slalom. The scientific knowledge of the size and course of external forces acting on a skier in this discipline is therefore poor. In recent kinematical studies, energy dissipation was derived from the centre of mass movement and related to kinematical movement characteristics. Energy dissipation, a measure for the quality of skiing, turned out having instantaneous statistical relations to key movement characteristics as well as to ranges of motion and performance measured in time. However scientific studies addressing this relation from a functional perspective, investigating how movement characteristics are related to kinetics and energy dissipation are lacking in the literature. The present study investigated the size and time course of the external forces acting on slalom skiers in direction of travel and the relation of the braking forces to energy dissipation. The kinematics of 6 members of the Norwegian Europa Cup team (aged 17-20) was captured during two turns of a slalom race simulation. External forces acting in the direction of travel were modelled based on kinematics and snow surface geomorphology. Energy dissipation was computed from the COM position and showed a strong inverse statistical correlation with the frictional force acting in the ski snow interaction ($R^2 = -0.96$, $p < 0.001$). The air drag force and the component of gravity pulling the skier downhill remained rather constant, while the size of the frictional force in the ski snow interaction altered to large extent throughout the turn cycle.

Key words: Alpine Skiing, Slalom, External Forces, Energy Dissipation.

Introduction

Few studies have addressed the modelling of external forces acting on the skier in the direction of travel. In two studies such forces were modelled for straight running situations (Kaps et al., 2005; Kaps et al., 1996) while four other studies have computed the external forces acting on a skier for turning situations (Lüthi et al., 2004; Ducret et al., 2004; Schiestl et al., 2006; Schiestl et al., 2005). None however related the external forces to energy dissipation (Supej *et al*., 2005). Energy dissipation is a measure for skiing quality, indicating the amount of total mechanical energy of the skier being lost to the environmental surrounding per meter altitude and kilogram body weight, by dissipative forces, such as air drag and ski-snow friction. Supej, (Supej *et al.,* 2004; Supej *et al.,* 2005; Supej *et al*., 2008) showed this measure being appropriate for the analysis of alpine skiing, since it allows instantaneous measures based on the centre of mass (COM) motion. On the data used for this study strong statistical relations between the range of vertical movement (Moger et al., 2007), the average fore / aft position during a turn cycle (Tjørhom et al., 2007) and performance measured in time were shown. Further, energy dissipation had a reasonable statistical relation to the fore / aft dynamics (Reid et al., 2008) and to the COM turn radius (Gilgien et al., 2007). The findings from these data give reason to believe that the underlying kinetics play an important role in the relation between movement and energy dissipation. However, scientific studies addressing this relation from a functional perspective, investigating how movement characteristics are related to kinetics and energy dissipation are lacking in the literature. The present study therefore foremost attempts to broaden the knowledge about the external forces acting on the skier in direction of travel in the discipline slalom. Further the relation between these forces and energy dissipation is investigated to establish a basis for the description how movements are related with kinetics and energy dissipation.

Methods

The kinematics of six male skiers aged 17 to 20 and belonging to the Norwegian Europa Cup team were analyzed through two complete turn cycles while conducting a slalom race simulation. A uniform course with gate distances and off-sets of 10 respectively 3m was set on an even inclined slope (on average 18˚) Snow conditions were hard and stable during the whole data collection. A skier's model based on joint centre and ski positions in space was computed using a DLT-based method and 4 panning cameras (50 Hz) (Mössner, Kaps, & Nachbauer, 1996; Nachbauer *et al*. 1996). The time-synchronisation of cameras was post-conducted by an adaptation of the software genlock method (Pourcelot, Audigié, Degueurce, Geiger & Denoix, 2000). To enable the DLT (Schiestl, 2005) transformation a calibration volume of approximately 50 x 10 x 2 m was spanned by two hundred and eight control points. The position of the control points and the snow surface were geodetically captured using a theodolite. Every camera frame was calibrated individually using in average 29 and minimal 14 control points. For transformation and digitization a costum application was developed in Matlab (TheMathWorks, Inc., Natick, MA.) yielding an 18 segment model based on 23 tracked points. The estimation of body segment parameters was based on Zatsiorsky's (2002) model using the de Leva (1996) adjustments. DLT-transformed position data were filtered by a 2nd order Butterworth filter with a cut-off frequency of 10 Hz for position data and 5 Hz for the centre of mass (COM) on which velocity and acceleration measures were based. Energy dissipation (Supej *et al*., 2005) was calculated based on the change in total mechanical energy (*ME*) per change in altitude of the COM per kilogram body mass (*m*) using finite central differences at each instant in time. Kinetic energy *(KE)* was based on the COM velocity ($v_{\_COM}$) and the potential energy *(PE)* on the COM altitude.

$$\begin{aligned} ME &= PE + KE \quad [J] \\ &= mgh + \frac{1}{2}mv^2 \quad [J] \\ E_{diss} &= \frac{\Delta ME}{m\Delta h} \quad [J \cdot kg^{-1} \cdot m^{-1}] \end{aligned}$$

Equation 1

In contrast to Supej's publications, the sign of E_{diss} was not changed according to stay in line with its physical definition. The turn cycle was divided by gate passage and transition which was defined as where the *COM* trajectory crosses the average ski trajectory projected onto the plane of the snow surface (Supej et al., 2003). The snow surface was modelled based on the terrestrially captured points by Delauney triangulation (de Berg et al., 2008) and a bi-cubic spline function for surface smoothing (Hugentobler, 2004; Watson, 1993; Sandwell, 1987). Local gradients were derived and the average angle between the main course direction and the average gradient calculated (14.5º). The external forces acting on the skier in the direction of travel are described by equation 2 consisting of the resultant force component in direction of travel ($F_{resultant}$), the component of gravity pulling the skier downhill (F_{slope}), the wind drag force (F_{drag}) and the frictional force occurring in the ski snow interaction ($F_{friction}$). Since the captured data are not suitable for the direct computation of $F_{friction}$ its size was determined by the rearrangement of equation 2 shown in equation 3.

$$F_{resultant} = F_{slope} + F_{drag} + F_{friction}$$

Equation 2

$$F_{friction} = F_{resultant} - F_{slope} - F_{drag}$$

Equation 3

Three different models for the computation of F_{slope} *and* $F_{resultant}$ were defined and their resulting forces compared. For model 1, F_{slope} *and* $F_{resultant}$ were derived as components of the total resultant force along the COM velocity vector, named F_{slope_COM} *and* $F_{resultant\_COM\_travel}$. In model 2, the skier was considered being rigid in direction normal to the local snow surface. $F_{resultant\_||}$ was defined as the component of $F_{resultant\_COM\_travel}$ being parallel to the local snow surface, and $F_{slope\_COM\_projected}$ was defined by the angle between the horizontal and the inclination of the slope in the direction of the velocity vector's normal projection on the local snow surface. In model 3, F_{slope_SKI} was defined as the direction vector of the modelled intersection point between the resultant ground reaction force and the local snow surface (PFA). The PFA modelling was based on the tip and tail positions of the skis and pressure distribution data between in and outside ski (Lüthi et al., 2004; Klous et al., 2008; Müller et al., 2005).For the computation of F_{drag} the simple frontal area equation was used, given in equation 4.

$$F_{drag} = c_d \cdot \frac{\rho \cdot v^2}{2} \cdot A$$

Equation 4

The drag coefficient, c_d was adapted from a study using cross country skiers of comparable body mass and clothing (Spring et al., 1988a) and computed dependent on the body posture in direction normal to the snow surface, accounting to some extent for alteration in body shape. Density, μ was calculated by the mean of meteorological measurements. Local wind velocity during data collection was not measured, but estimated from meteorological data captured at a station 20km from the place of investigation and qualitative observation on site. The instantaneous, 3-dimensional COM velocity ($v_{\_COM}$), adjusted for 1m/s constant headwind, was used for the relative air velocity around the skier. The frontal area was modelled by attaching volumes to the 18 segments skier model and its orthographic projecting into a plane normal to $v_{\_COM}$. A pixel counting function (Brodie, 2008) was finally used to estimate the instantaneous area of the projected volume. As measure for movement characteristics, the distance between COM and its normal projection into the local snow surface (d_{COM_SS}) was computed as well as the projection of the angle spanned by the velocity vectors of *PFA* and COM onto the snow surface ($angle_{COM\_PFA}$). Further the distance between PFA and its projection into the plane normal to $v_{\_COM}$ vector was computed as a measure for the relative fore aft movement of the skis relative to the COM.

Results

Figure 1, shows the time course of the ensemble average forces for the 6 skiers during the two consecutive turns. The bird's eye view on the skier's trajectory corresponds with gate and transition passages in the force graph. An arrow indicates the gradient vector spanning an angle of 14.5º to the main course direction.

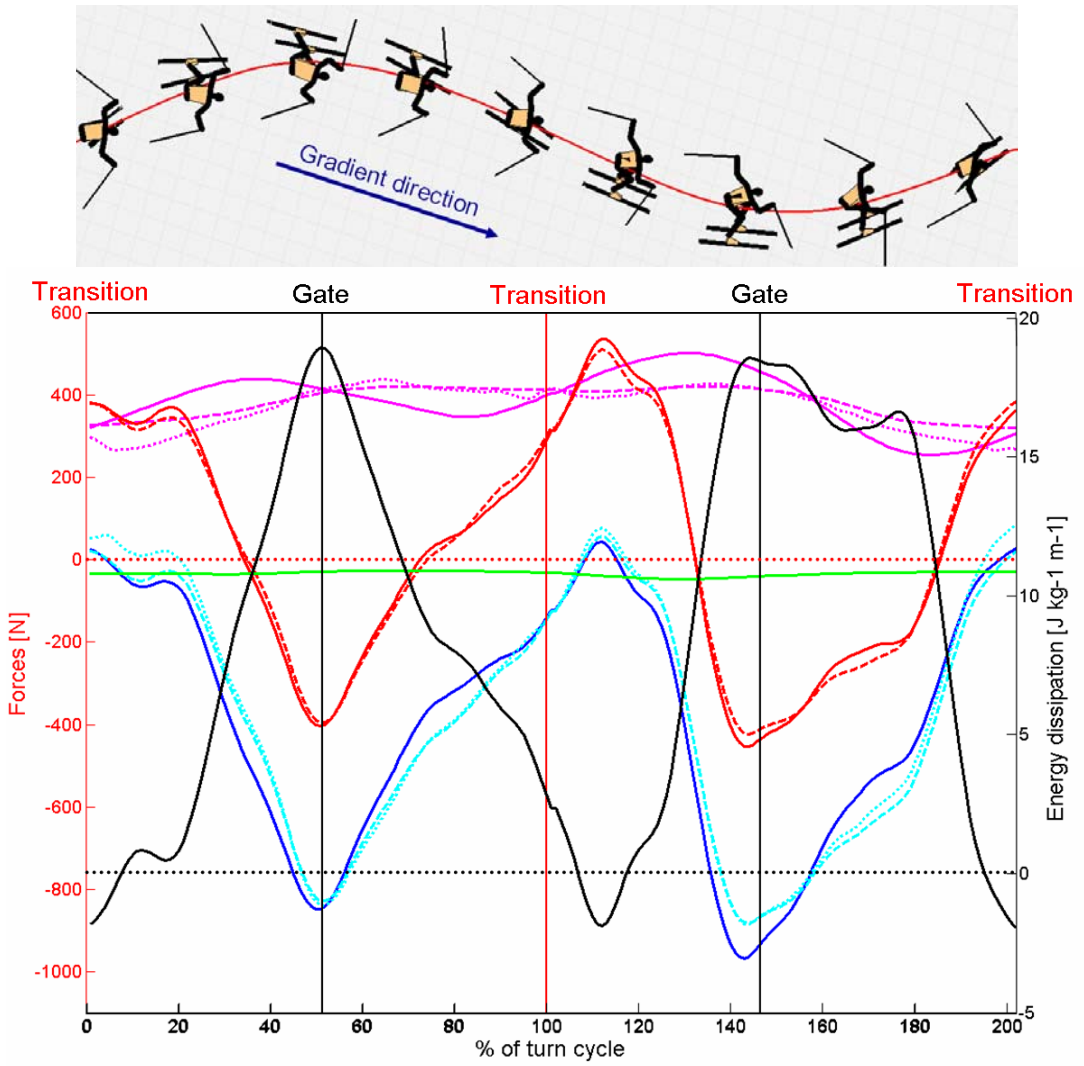

Figure1: Ensemble average curves of 6 skiers through 2 turns: energy dissipation: black, $F_{resultant\_travel}$: red solid, $F_{resultant\_||}$: red dashed, $F_{friction\_1}$: dark blue, $F_{friction\_2}$: blue dashed, $F_{friction\_3}$: blue dotted, F_{slope_COM}: pink solid, $F_{slope\_COM\_projected}$: pink dashed, F_{slope_SKI}: pink dotted.

The right side axis corresponds to energy dissipation where the ensemble average curve is given in black. The forces, referring to the left hand side axis are plotted such, that the braking forces $F_{\_drag}$ *and* $F_{friction}$ appear negative and the accelerating force F_{slope}

positive. If the magnitude of $F_{resultant}$ is plotted positive, the skier is accelerated in the direction of travel. Depending on the choice of the model and the skier's angle to the gradient, F_{slope} ranges from 250 to 500 N. The peak forces are reached while skiing close to parallel with the gradient between the gates. Apparently, vertical movement normal to the snow surface (d_{COM_SS}) included in the computation of F_{slope_COM} but excluded in model 2 and 3 ($F_{slope\_COM\_projected}$ *and* F_{slope_SKI}) contributes significantly to the magnitude of F_{slope}. Decreasing d_{COM_SS} towards the gate passage increases F_{slope_COM} significantly in that section of the turn, while F_{slope_COM} is decreased due to the relative elevation of the COM from gate passage to turn transition. Comparing $F_{slope\_COM\_projected}$ *and* F_{slope_SKI} it is apparent, that F_{slope_SKI} is decreased when the PFA vector is spanning a larger angle to the gradient than the COM vector does before the first and after the second gate. When travelling along the direction of the gradient their size is roughly similar. Within the models limitations the dissipative force due to air resistance is small and relatively constant compared to the braking force in the ski snow interaction. Its ensemble average time course during the turns is given by the solid red line in the graph below.

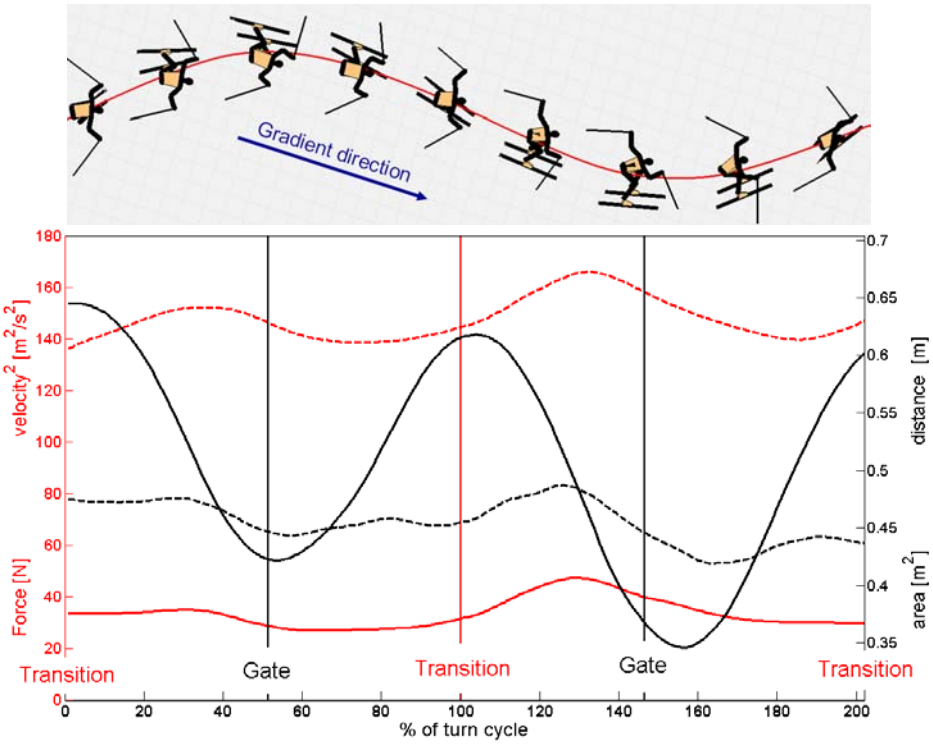

Figure2: Ensemble average curves of 6 skiers through 2 turns: F_{drag}: red solid, $v_{COM}2$: red dashed, d_{COM_SS}: black solid, frontal area: black dashed.

F_{drag} is largest between the second transition and second gate, when the frontal area opposed to the air is maximal at the same time as velocity is maximal due to the precedent travel along the direction of the gradient.

$F_{resultant}$ is maximal during the straight running phase after the transition and minimal at about gate passage. The vertical movement normal to the snow surface included in $F_{resultant\_travel}$ contributes little to the total resultant force. The average root-mean-square difference between the ensemble average $F_{resultant\_travel}$ and $F_{resultant\_||}$ is 18.4 N and the maximal difference between their ensemble average forces was 35.8N.

The braking force in the ski snow interaction ($F_{friction}$) varies substantially during the time course of the two turns. It is maximal at about the gate passage and minimal at the transition between the turns. $F_{friction}$ is larger in the end of the second turn, when the COM velocity vector of the skier spans a larger angle to the gradient, than at the end of the first turn. Right after turn transition its values indicate a propulsive force in the direction of travel from the ski snow interaction to the skier. This propulsive force is larger for the second and third force model than for the first one. Comparing F_{slope}, $F_{friction}$ and $F_{resultant}$ based on the three models, substantial differences are found in F_{slope} and $F_{friction}$, which are mainly caused by the calculation method used for F_{slope} computation.

Table 1: Root-mean-square differences and maximal differences between the ensemble average F_{slope_COM}, $F_{slope\_COM\_projected}$, F_{slope_SKI}.

rms [N] / max [N]	F_{slope_COM}	$F_{slope\_COM\_projected}$	F_{slope_SKI}
$F_{slope\_COM\_projected}$	47.5 / 81.9		18.7 / 62.1
F_{slope_SKI}	50.5 / 98.3	18.7 / 62.1	

Table 2: Root-mean-square differences and maximal differences between the ensemble average $F_{friction\_1}$, $F_{friction\_1}$ and $F_{friction\_1}$.

rms [N] / max [N]	$F_{friction\_1}$	$F_{friction\_2}$	$F_{friction\_3}$
$F_{friction\_2}$	48.4 / 103.3		20.8 / 68.2
$F_{friction\_3}$	53.5 / 77.5	20.8 / 68.2	

E_{diss} showed a strong statistical relation on the ensemble average data of the 6 skiers with $F_{friction}$ (R^2 = -0.96, p < 0.001), but no relation with F_{drag} (R^2 = 0.20, p<0.5). E_{diss} is negative, indicating an increase in ME during the same periods $F_{friction}$ indicates a propulsive force from the ski snow interaction.

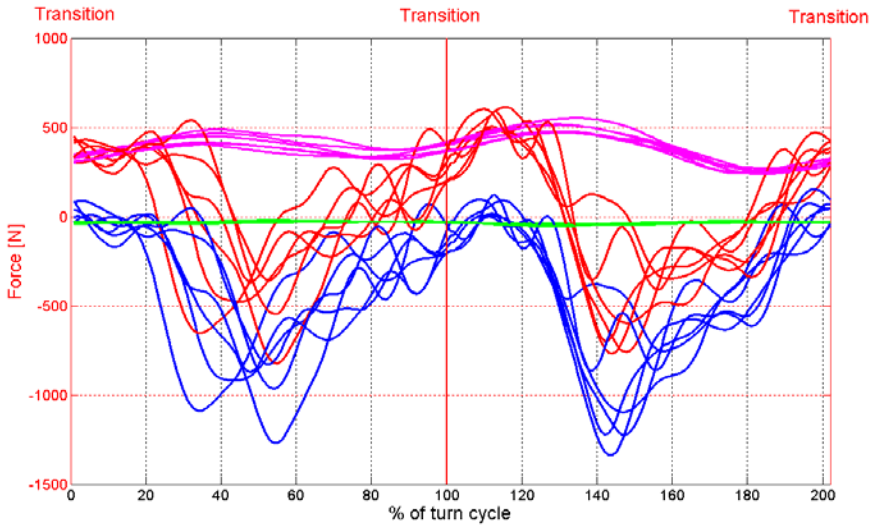

Figure 4: Force curves of the 6 skiers through 2 turns: $F_{resultant\_travel}$: red, $F_{friction\_1}$: dark blue, F_{slope_COM}: pink.

The graph above shows the variability of the forces acting on the 6 skiers. It is apparent, that turn 1, turning towards the direction of the gradient yield larger variability in terms of timing of $F_{friction}$ than the second turn, digressing from the direction of the gradient. Figure 5, shows the skier with the smallest total propulsive impulse computed from the positive $F_{friction}$ values during the post-transition phase ($F_{friction}$_+_phase). Graph C within figure 5 indicates, that $v_{\_COM}$ is maximal before the second gate, when the slope inclination is larger during the turn transition than before the first gate. Regarding the $F_{friction}$_+_phase graph B and C show, that the $angle_{COM\_PFA}$ and v_{COM_PFA} are maximal d_{COM_SS} starts decreasing when $F_{friction}$ is indicating a propulsive force on the skier.

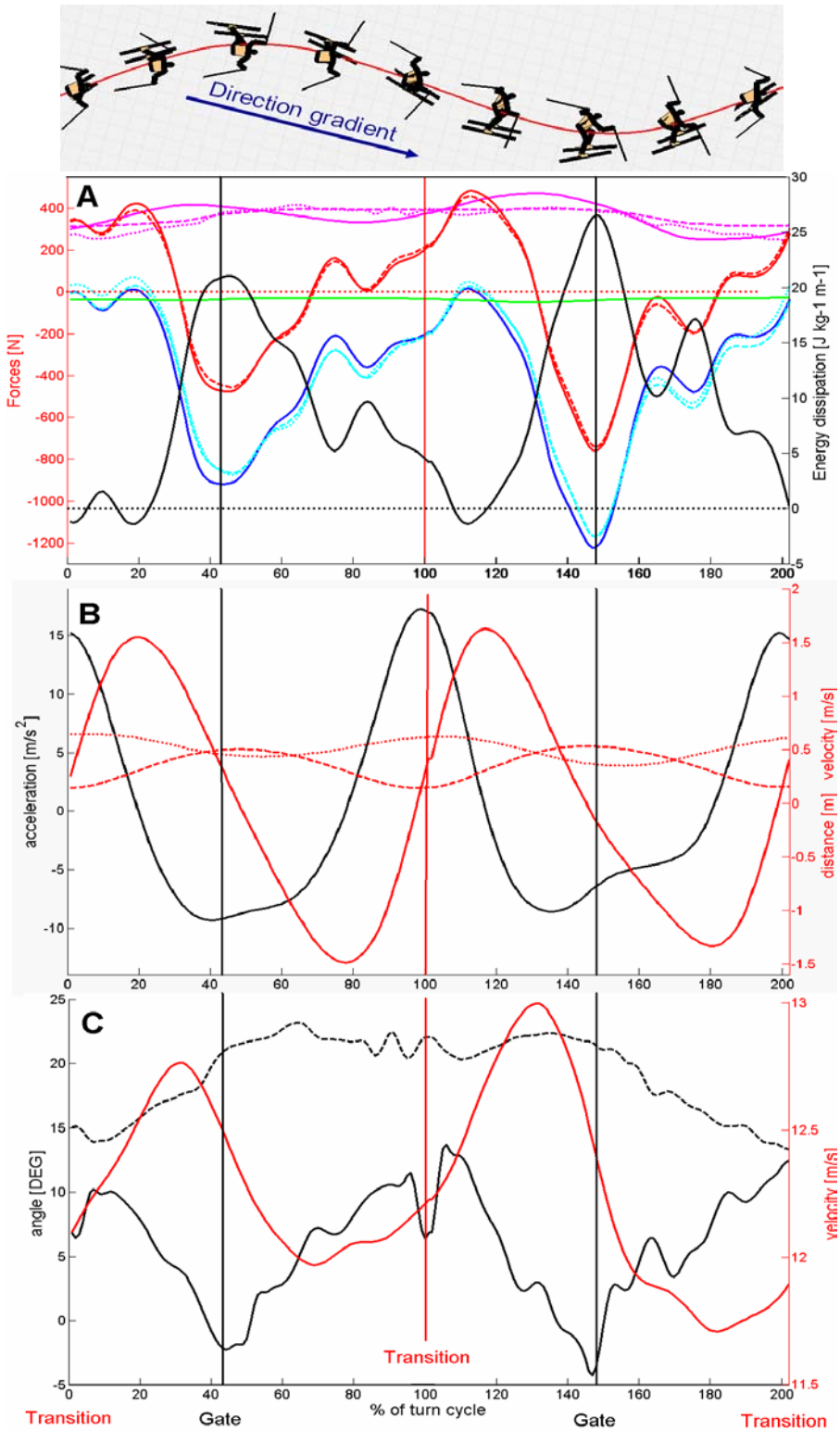

Figure 5: Graph A: energy dissipation: black, $F_{resultant\_travel}$: red solid, $F_{resultant\_travel}$: red dashed, $F_{friction\_1}$: dark blue, $F_{friction\_2}$: blue dashed, $F_{friction\_3}$: blue dotted, F_{slope_COM}: pink solid, $F_{slope\_COM\_projected}$: pink dashed, F_{slope_SKI}:pink dotted. Graph B: , a_{COM_PFA}: black, v_{COM_PFA}: red solid, d_{COM_PFA}: red dashed, d_{COM_SS}: red dotted. Graph C: v_{COM}: red, $angle_{COM\_PFA}$: black solid, slope inclination in direction of PFA vector: black dashed.

Discussion

The comparison of the force computations based on the three models show substantial differences in F_{slope}. The main differences occur, when F_{slope_SKI} is extensively decreased compared to the other forces, during the period the instantaneous PFA velocity vector spans a larger angle with the gradient than with the other F_{slope} model forces during the period of transition from left to right turns until gate passage. Further, the extensive differences occur due to the contribution of the vertical movement normal to the snow surface to the first models component of gravity, F_{slope_COM}. The component of F_{slope} added by movement normal to the snow surface is given by the difference between F_{slope_COM} and $F_{slope\_COM\_projected}$. These differences in F_{slope} affect the whole force composition, since the summation equation 2 and 3 are not over determined. Therefore the force models need to be discussed from a functional perspective: Envisioning a skier running straight along the gradient crossing a medium sized bump lying in transversal direction to the skier's trajectory across the hill. Force model 2 computes F_{slope} for this situation based on the instantaneous slope inclination and considers the skier being rigid with the COM in a constant distance from the snow surface, even if the skier bends his knee and hip joints, when passing the bump, to flatten his COM trajectory in vertical dimension. From that perspective model 1 seems being superior, since it accounts for relative alterations in ski and COM trajectories, at least in vertical direction. Model 3 might contribute to the understanding of the difference between the components of gravity acting on the COM and the skis. We conclude that the differences in size between the three models computed forces are such substantial, that further investigation is needed.

Regarding the overtopping of $F_{resultant}$ relative to F_{slope}, the accuracy of the slope inclination measurement has to be questioned, since F_{slope} is directly dependent on the accuracy of that measure. Based on model calculations the inclination of the component of gravity pulling the skier downhill needed to be 6º to 7º steeper to equal F_{slope} with $F_{resultant}$ of the largest forces measured for individual skiers. To reduce the difference between F_{slope} and $F_{resultant}$ in force model 1, 6º are needed while it is 7º for the other models. Since the position measurement with the theodolite was conducted from one place only it is unfortunately impossible to justify whether it was standing truly vertical.

Since its vertical axis was controlled frequently during the measurement process and no shift over time was registered, only a false alignment between the theodolite's vertical axis and level remains as source for such an error. Since the owner of the theodolite controls the axis alignment and has not reported a failure, it seems improbable, that an error in the vertical axis alignment of 6º to 7º has occurred. Some systematic error is naturally present, but probably not as large as 6 to 7º. Since there is no possibility for justification, we suggest for future data collections to base the inclination measurement on a polygon-net of basis points around the area of investigation to enable the control for such error. Regarding the limitations of the wind drag force computation, the systematic error needed to be beyond 100% of the total drag force to reduce $F_{friction}$ exclusively indicating de-accelerating forces during the whole course. We have not investigated whether the choice of the body segment parameter model could be affecting the computation of $F_{resultant}$. In case the model would overestimate the mass of the lower extremities, a forward movement of the legs relative to the upper body could cause an overestimation of the forward movement of the COM in direction of travel and lead to a temporally limited increase in velocity of the COM. Potentially the overreaching of $F_{resultant}$ over F_{slope} during the $F_{friction_+}$_phases could be caused by a summation of errors in the alignment of the vertical axis of the theodolite, the F_{drag} and F_{slope} modelling and a errorneous estimation of the body segment parameters. In case the overtopping of $F_{resultant}$ over F_{slope} during the $F_{friction_+}$_phases is not caused by failure in the methods but real, this finding could contribute to the question whether athletes are able to increase velocity due to muscular work. This topic was brought into scientific discussion by Lind and Sanders (Lind & Sanders, 2003) arguing that the kinetic energy of a skier can be increased by increase of the angular velocity by body extension while leaning towards the centre of the turn. Supej (Supej, 2003) argued it being impossible to conduct a substantial explosive body extension during turning, due to the ground reaction forces being too high to allow such a movement. Our finding that $F_{resultant}$ overreaches F_{slope} does not require the mechanism discussed by Lind and Supej, since the section the phenomenon occur is different. The discussion about increasing kinetic energy due to increased angular velocity refers to the turning phase when the turn radii are low, while $F_{resultant}$ overreaching F_{slope} in our data occurs after the transition in the so called $F_{friction_+}$_phase. In this phase, the skis have crossed the COM trajectory to the new outside of the upcoming turn and the skier is about to be

accelerated to maximal velocity. Further, the skier is slightly increasing d_{COM_PFA}, has started to reduce the distance of the COM normal to the snow surface and is leaning the body slightly to the inside of the turn. The angle between the COM trajectory and the gradient projected onto the snow surface is smaller than the angle between the PFA direction vector and the gradient as figure 7 illustrates. These geometry properties are true for both turning directions.

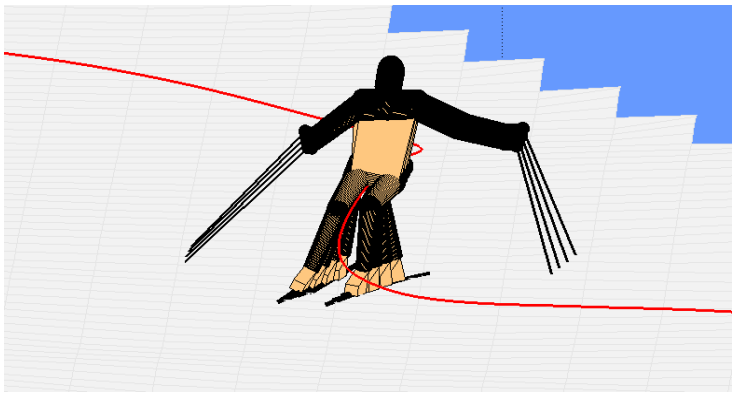

Figure 6: Illustration of 4 frames during which $F_{resultant}$ is larger than F_{slope}.

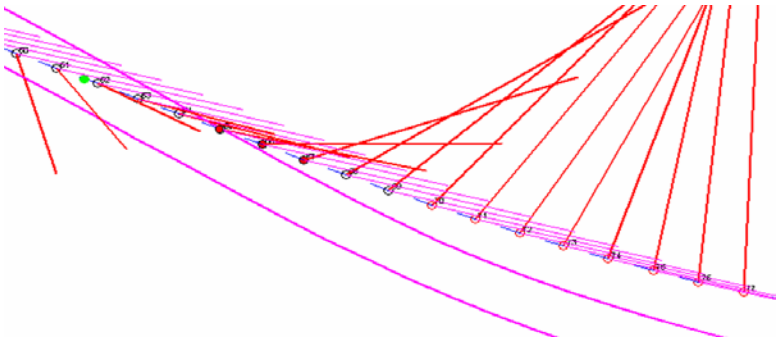

Figure 7 : Bird eye perspective on post transition phase: Ankle joint trajectory: thick pink lines, direction of gradient: thin pink line: Resultant force vector: red, COM positions: circles, transition point: green, COM position for situations when $F_{resultant}>F_{slope}$: red dot.

The angle spanned by the ski- and COM direction vectors and the slight forward motion of the skis relative to the COM belong to a movement that eventually could cause propulsion, if a force component normal the skis is produced. Since the angle between ski- and COM direction is rather small I doubt this movement being the only reason for the additional forward propulsion. Considering the skier divided into skis/lower legs and upper body, the upper body is to larger extent affected by gravity than the lower part of the body, due to their different angle of the velocity vector to gravity. These indicate what the propulsive force sourced in the ski snow interaction could be based

on. We are unable to give the reason for the eventual propulsion from ski/snow interaction occurring during that phase of the turn, further investigation is needed. However, the fact that energy dissipation is negative around transition is confirmed by these data and it is further indicated a relation to the propulsive force. The reason for this to occur is probably based on the skier's movement characteristics which are consistently present for all skiers during the given phase in the turn cycle.

Despite the models limitations, we can confirm, that the air drag force is of minor importance in slalom compared to $F_{friction}$ and the importance of air drag in the speed disciplines. A more precise estimate of F_{drag} needs to be computed by wind tunnel testing, since the drag coefficient is most probably changing within the speed range typical for slalom and with body posture. Wind measurements were not taken during the data collection since external force modelling was not the projects intention at that status of the project, but needs to be conducted during future data collections.

References

Reference List

Abdel-Aziz, Y. I. & Karara, H. M. (1971). *Direct linear transformation from comparator coordinates into object space coordinates in close-range photogrammetry*. In *Symposium on Close-Range Photogrammetry* (pp. 1-18). Falls Church: American Society of Photogrammetry.

Barelle, C., Ruby, A., & Tavernier, M. (2004). *Experimental Model of the Aerodynamic Drag Coefficient in Alpine Skiing*. *Journal of Applied Biomechanics, 20,* 167-176.

Brodie, M. (28-10-2008). *Pixel counting algorithm to estimate wind drag.* Ref Type: Personal Communication

Chen, L., Armstrong, C. W., & Raftopoulos, D. D. (1994). *An investigation on the accuracy of three-dimensional space reconstruction using the direct linear transformation technique*. *Journal of Biomechanics, 27,* 493-500.

de Berg, M., Otfried, C., van Kreveld, M., & Overmars, M. (2008). *Computational Geometry: Algorithms and Applications*.

de Leva, P. (1996). *Adjustments to zatsiorsky-seluyanov's segment inertia parameters*. *Journal of Biomechanics, 29,* 1223-1230.

Gilgien, M., Reid, R., Haugen, P., & Smith, G. (2008). *Digital terrain modelling of snow surfaces for use in biomechanical investigations in snow sports.* In *13th Annual Congress of the European College of Sport Science*.

Gilgien, M., Reid, R., Tjørhom, H., Moger, T., Haugen, P., Kipp, R. et al. (2007). *Energy dissipation and slalom turn radius.* In *4th International Congress on Science and Skiing 2007* Salzburg, Austria: E. Müller, S. Lindinger, T. Stöggl, & V. Fastenbauer.

Gorlin, M., Maseev, W., Zyrjanov, W., & Remizov, L. (1987). *Sliding friction and boundary lubrication of snow*. *Journal of Tribology, 109,* 614-617.

Habel, B. (1968). *Über die Bestimmung von Luftwiderstand und Gleitreibung beim Skilauf. Europa Sport, 20,* 950-955.

Haugen, P., Reid, R., Tjørhom, H., Moger, T., Gilgien, M., Kipp, R. et al. (2007). *Centre of mass velocity and the turn cycle in slalom.* In *4th International Congress on Science in Skiing*.

Howe, H. (2001). *The New Skiing Mechanics*.

Hugentobler, M. (2004). *Terrain Modelling with Triangle Based Free-Form Surfaces.* ETH Zurich, Switzerland.

Kaps, P., Nachbauer, W., & Mossner, M. (2005). *Snow friction and drag in alpine downhill racing.*

Ref Type: Unpublished Work

Kaps, P., Nachbauer, W., & Mossner, M. (1996). *Determination of kinetic friction and drag area in alpine skiing*. In C.D.Mote, R. J. Johnson, W. Hauser, & P. S. Schaff (Eds.), *Ski Trauma and Skiing Safety: 10th Volume* (Philadelphia: American Society for Testing and Materials.

Klous, M., Müller, E., & Schwameder, H. (2008). *Knee joint loading an alpine skiing: A comparison between carved and skikked turns*. In *12th Annual Congress of the European College of Sport Science*.

Leino, M. & Spring, E. (1984). *Determination of the coefficient of kinetic friction between ski and snow from gliding velocity of a skier*. *Geophysics, 19*.

LeMaster, R. (1999). *The skiers edge*. Human Kinetics.

Lind, D. & Sanders, S. (2003). *The Physics of skiing*. (2nd ed.) New York: Springer.

Luethi, S. & Denoth, J. (1987). *The Influence of Aerodynamic and Anthropometric Factors on Speed in Skiing*. *International Journal of Sport Biomechanics, 3,* 345-352.

Lüthi, A., Federolf, P., Fauve, M., Oberhofer, K., Rhyner, H., Amman, W. et al. (2004). *Determination of forces in carving using three independent methods.* In D. Bacharach & J. Seifert (Eds.), *3rd International Congress on Skiing and Science* (pp. 3-4). St. Cloud State University.

Malberg, H. (2002). *Meteorologie und Klimatologie: Eine Einführung*. Springer.

Moger, T., Reid, R., Haugen, P., Tjørhom, H., Gilgien, M., & Smith, G. (2007). *Kan en ved hjelp av en 3 dimensjonal kinematisk analyse beskrive tyngdepunktsbanen til*

SL - løpere nøyaktig nok til å beskrive viktige prestasjonskarakteristika til tyngepunktsbanen? Norwegian School for Sport Science, Oslo, Norway.

Mossner, M., Kaps, P., & Nachbauer, W. (1996). *A method for obtaining 3-d data in alpine skiing using pan-and-tilt cameras with zoom lenses.* In C.D.Mote, R. J. Johnson, W. Hauser, & P. S. Schaff (Eds.), *Skiing Trauma and Safety: Tenth Volume* (pp. 155-164). Philadelphia: American Society for Testing and Materials.

Müller, E., Schiefermuller, C., Kröll, J., & Schwameder, H. (2005). *Skiing with carving skis - what is new?* In E.Müller, D. Bacharach, R. Klika, S. Lindinger, & H. Schwameder (Eds.), *3rd International Congress on Skiing and Science* (pp. 15-23). Oxford: Meyer & Meyer Sport.

Nachbauer, W., Kaps, P., Nigg, B., Brunner, F., Lutz, A., Obkircher, G. et al. (1996). *A video technique for obtaining 3-d coordinates in alpine skiing. Journal of Applied Biomechanics, 12,* 104-115.

Pourcelot, P., Audigie, F., Degueurce, C., Geiger, D., & Denoix, J. M. (2000). *A method to synchronize cameras using the direct linear transformation technique. Journal of Biomechanics, 33,* 1751-1754.

Reid, R., Gilgien, M., Moger, T., Tjørhom, H., Haugen, P., Kipp, R. et al. (2008). *Turn characteristics and energy dissipation in slalom.* In *4th International Congress on Science and Skiing 2007* Salzburg, Austria: E. Müller, S. Lindinger, T. Stöggl, & V. Fastenbauer.

Reid, R., Tjørhom, H., Moger, T., Haugen, P., Kipp, R., & Smith, G. (2007). *Accuracy od 3d position prediction over a large object space using pan and tilt cameras.* In *12th Annual Congress of the European College of Sport Science*.

Sandwell, T. (1987). *Biharmonic Spline Interpolation of GEOS-3 and SEASAT Altimeter Data. Geophysical research letters, 14,* 139-142.

Schiestl, M. (2005). *Improving DLT precision with constant camera parameters.* Ref Type: Unpublished Work

Schiestl, M., Kaps, P., Mossner, M., & Nachbauer, W. (2005). *Snow friction and drag during the downhill race in Kitzbuhel.* In *Mountain and sport: Updating study and research from laboratory to field* (pp. 54).

Schiestl, M., Kaps, P., Mossner, M., & Nachbauer, W. (2006). *Calculation of friction and reaction forces during an alpine world cup downhill race.* In E.F.Moritz & S. Haake (Eds.), *The engineering of sport 6, Volume 1: Developments for sports* (pp. 269-274). New York: Springer.

Shapiro, R. (1978). *Direct linear transformation method for three-dimensional cinematography. Research Quarterly, 49,* 197-205.

Spring, E., Savolainen, S., Erikkila, T., Hamalainen, T., & Pihkala, P. (1988). *Drag area of a crosscountry skier. International Journal of Sport Biomechanics, 4,* 103-113.

Supej, M. (2003). *The myth of acceleration and push-off in racing alpine skiing.* Ref Type: Unpublished Work

Supej, M. (2008). *Differential specific mechanical energy as a quality parameter in racing alpine skiing. Journal of Applied Biomechanics*.

Supej, M., Kugovnik, O., & Nemec, B. (2005). *Energy principle used for estimating the quality of a racing ski turn.* In E. Müller, D. Bacharach, S. Klika, S. Lindinger, & H. Schwameder (Eds.), *3rd international congress on science in skiing* (pp. 228-237). Adelaide: Meyer & Meyer Sport Ltd..

Supej, M., Kugovnik, O., & Nemec, B. (2003). *Kinematic determination of the beginning of a ski turn*. *Kinesiologia Slovenica, 9,* 11-17.

Supej, M., Kugovnik, O., & Nemec, B. (2004). *The energy principle used for estimating the quality of the racing ski turn.* In D. Bacharach & J. Seifert (Eds.), *3rd International Congress on Skiing and Science* (pp. 63-64). St. Cloud State University.

Tjørhom, H., Reid, R., Haugen, P., Moger, T., Gilgien, M., & Smith, G. (2007). *Beskrivelse av tyngdepunktets frem/bak dynamikk i slalåm sett opp mot prestasjon ved hjelp av en 3 dimensjonal kinematisk analyse.* Norwegian School for Sport Science, Oslo, Norway.

Watson, D. F. (1993). *Contouring: a guide to the analysis and display of spatial data. Computers & Geosciences, 19,* 1389-1391.

Wood, G. A. & Marshall, R. N. (1986). *The accuracy of dlt extrapolation in three-dimensional film analysis*. *Journal of Biomechanics, 19,* 781-785.

Zatsiorsky, V. M. (2002). *Kinetics of human motion*. Champaign: Human Kinetics, Inc.

Zatsiorsky, V. M. & Seluyanov, V. (1985). *Estimation of the mass and intertia characteristics of the human body by means of the best predictive regression equations*.

5. Appendix

Table1: *Meteorological data from the weather station Gardermoen, 18 km north-west from the data collection area.*

4780	GARDERMOEN			202	60,2	11,1	ULLENSAKER					
							AKERSHUS					
							ØSTLANDET					
Kode	Navn	Enhet										
DD06	Vindretning kl. 06 UTC	grader										
FFM	Middel vindhastigheter	m/s										
POM	Midlere lufttrykk st.	hPa										
PON	Laveste lufttrykk st.	hPa										
POX	Høyeste lufttrykk st.	hPa										
TAM	Middeltemperatur	C										
TAN	Minimumstemperatur	C										
TAX	Maksimumstemperatur	C										
UUM	Midl. Rel. luftfuktighet	%										
UUN	Min. rel. luftfuktighet	%										
UUX	Maks. rel. luftfuktighet	%										
VP	Vanndamptrykk	hPa										
4780 GARDERMOEN April 2006												
Dato	DD06	FFM	POM	PON	POX	TAM	TAN	TAX	UUM	UUN	UUX	VP
10	320	4,1	985	983	987	2,9	-1,8	6,7	59	50	69	4,5
11	30	3,8	985	983	987	0	-5,8	5,5	81	59	85	4,9
12	**150**	**3,1**	**979**	**978**	**980**	**1,2**	**0,3**	**2,4**	**99**	**93**	**100**	**6,5**